Nonlinear state observation using H_∞-filtering Riccati design

Reif, K. Sonnemann, F. Unbehauen, R.
BMW AG, Munich, Germany;

This paper appears in: **Automatic Control, IEEE Transactions on**

Publication Date: Jan. 1999
On page(s): 203 - 208
Volume: 44 , Issue: 1
ISSN: 0018-9286
Reference Cited: 22
CODEN: IETAA9
Inspec Accession Number: 6138200

Abstract:
The authors propose an observer for continuous-time nonlinear systems. The observer gain is computed by a **Riccati** differential equation similar to the extended Kalman filter. They prove that under certain conditions the proposed observer is an exponential observer by choosing an appropriate Lyapunov function. Furthermore, the authors explore some important relations of the proposed observer to robust control theory and H_∞-filtering. To examine the practical usefulness of the proposed observer they applied it to an induction **motor** for the estimation of the rotor flux and the angular velocity

Index Terms:
Kalman filters Lyapunov methods **Riccati** equations continuous time systems differential equations filtering theory induction **motors** nonlinear systems observers robust control $H_{\&infin}$ -filtering Lyapunov function **Riccati** differential equation angular velocity continuous-time systems extended Kalman filter induction **motor** nonlinear systems observer robust control rotor flux state observation

Reference list:
1, J.Baras, A.Bensoussan, and M. R.James, "Dynamic observers as asymptotic limits of recursive filters: Special cases," *SIAM J. Appl. Math.*, vol. 48, pp. 1147-1158, 1988.

2, T.Basar and B.Bernhard, *H_{∞}-Optimal Control and Related Minimax Design Problems* Boston, MA: Birkha¨user, 1995.

3, R. Y.Chiang and M. G.Safonov, *Robust Control Toolbox User's Guide* Natick, MA: The Mathworks, 1992.

4, J. C.Doyle, B. A.Francis, and A. R.Tannenbaum, *Feedback Control Theory*, New York: Macmillan, 1992.

5, A.Gelb, *Applied Optimal Estimation* Cambridge, MA: MIT Press, 1984.

6, M.Green and D. J. N.Limebeer, *Linear Robust Control* Englewood Cliffs, NJ: Prentice-Hall, 1995.

7, R. E.Kalman, "New methods in Wiener filtering theory," *Proc. 1st Symp. on Eng. Appl. of Random Function Theory and Probability*, J.Bogdanoff and F.Kozin, Ed. , New York: Wiley, pp. 270-388, 1963.

8, S. R.Kou, D. L.Elliott, and T. J.Tarn, "Exponential observers for nonlinear dynamic systems," *Inform. Contr.*, vol. 29, pp. 204-216, 1975.

9, P. P.Khargonekar, I. R.Petersen, and K.Zhou, "Robust stabilization of uncertain linear systems: Quadratic stabilizability and H_{∞} control theory," *IEEE Trans. Automat. Contr.*, vol. 35, pp. 356-361, 1990.
[Abstract] [PDF Full-Text (540KB)]

10, P. P.Khargonekar, "State space H_{∞} control theory and the LQG problem," *Mathematical System Theory*, A.Antoulas, Ed. , pp. 159-176, 1991.

11, H.Kwakernaak, "Robust control and H_{∞}-optimization," *Automatica*, vol. 29, pp. 255-273, 1993.

12, W.Leonhard, *Control of Electrical Drives* Berlin, Germany: Springer-Verlag, 1985.

13, E. A.Misawa and J. K.Hedrick, "Nonlinear observers—A state-of-the-art survey," *ASME J. Dyn. Syst. Meas. Contr.*, vol. 111, pp. 344-352, 1989.

14, K. M.Nagpal and P. P.Khargonekar, "Filtering and smoothing in a H_{∞}-setting," *IEEE Trans. Automat. Contr.*, vol. 36, pp. 152-166, 1991.
[Abstract] [PDF Full-Text (1160KB)]

15, G.Pfaff, *Regelung Elektrischer Antriebe I* Mu¨nchen, Germany: Oldenbourg Verlag, 1990.

16, K.Reif and R.Unbehauen, "Linearization along trajectories and the extended Kalman filter," *Proc. 13th IFAC World Congr.*, vol. H, pp. 509-514, 1996.

17, K.Reif, F.Sonnemann, and R.Unbehauen, "Modification of the extended Kalman filter with an additive term of instability," *Proc. 35th IEEE Conf. Decision and Control* Kobe, Japan, pp. 4058-4059, 1996.
[Abstract] [PDF Full-Text (160KB)]

18, K.Reif, "Steuerung von nichtlinearen systemen mit Homotopie-Verfahren," *Fortschritt-Berichte VDI* Du¨sseldorf, Germany: VDI-Verlag, vol. 8, 1997.

19, L.Salvatore, S.Stasi, and L.Tarchioni, "A new EKF-based algorithm for flux estimation in induction machines," *IEEE Trans. Ind. Electron.*, vol. 40, pp. 496-504, 1993. [Abstract] [PDF Full-Text (668KB)]

20, G.Tadmor, "Uncertain feedback loops and robustness in general linear systems," *Automatica*, vol. 27, pp. 1039-1042, 1991.

21, M.Vidyasagar, *Nonlinear Systems Analysis* Englewood Cliffs, NJ: Prentice-Hall, 1993.

22, B. L.Walcott, M. J.Corless, and S. H.Zak, "Comparative study of nonlinear state-observation techniques," *Int. J. Contr.*, vol. 45, pp. 2109-2132, 1987.

Search Results [PDF FULL-TEXT 196 KB] PREV NEXT DOWNLOAD CITATION

Home | Log-out | Journals | Conference Proceedings | Standards | Search by Author | Basic Search | Advanced Search | Join IEEE | Web Account | New this week | OPAC Linking Information | Your Feedback | Technical Support | Email Alerting | No Robots Please | Release Notes | IEEE Online Publications | Help | FAQ| Terms | Back to Top

Nonlinear State Observation Using H_∞-Filtering Riccati Design

Konrad Reif, Frank Sonnemann, and Rolf Unbehauen

Abstract— **In this paper, the authors propose an observer for continuous-time nonlinear systems. The observer gain is computed by a Riccati differential equation similar to the extended Kalman filter. They prove that under certain conditions the proposed observer is an exponential observer by choosing an appropriate Lyapunov function. Furthermore, the authors explore some important relations of the proposed observer to robust control theory and H_∞-filtering. To examine the practical usefulness of the proposed observer they applied it to an induction motor for the estimation of the rotor flux and the angular velocity.**

Index Terms— **Extended Kalman filter, H_∞-filtering, nonlinear observer.**

I. Introduction

The basic model for the general nonlinear observation problem consists of a nonlinear plant and a nonlinear output map, at which neither system noise nor observation noise is considered. The problem is to estimate the states of the plant by observing the output when the initial state of the plant is not known. In literature the design of nonlinear observers is a widespread area of current research (see [13] and [22] for a survey). Although many important results have been achieved, there are still possibilities for an improvement of the existing synthesis methods.

A frequently applied method is the extended Kalman filter [5], used as a deterministic observer for nonlinear systems. The advantage is its easy handling with a simultaneous good performance; moreover, a full proof of its exponential stability has been given recently [16], [18]. However, a well-known difficulty arising through its application is the problem of divergence. The reason is that in computation of the observer gain only the linearized functions are considered, but not the whole nonlinearities. To obtain convergence, it is therefore, in general, necessary either to have a good initial guess so that the initial estimation error is sufficiently small or to permit functions only weakly nonlinear [16], [18].

Recently H_∞-control methods have attracted attention in robust control theory [4], [11]. It has been mentioned that the high robustness of the LQ-optimal control systems can be further improved by using H_∞-control [3]. In this paper we use a similar approach to improve the extended Kalman filter. Motivated by the results of robust control theory [9], [20] and H_∞-filtering [2], [6], [10], [14]. The remaining nonlinear terms are treated as uncertainties and are implemented in the proposed observer design by a worst case valuation in such a way that these uncertainties can be tolerated. Consequently, better convergence properties can be expected; moreover, under certain conditions convergence can be achieved even independent of the initial estimation error. An alternative method for improving the convergence properties of the extended Kalman filter has been proposed in [17].

The paper is organized as follows: in Section II we state the necessary preliminaries and introduce the proposed nonlinear observer. By choosing an appropriate Lyapunov function we show that the proposed observer is an exponential observer in the sense of [8]. Important relations to H_∞-filtering [2], [6], [10], [14] are explored in Section III. In Section IV we apply the proposed observer to estimate the rotor flux and the angular velocity of an induction motor (cf. [12], [15], [19]). Some conclusions are drawn in Section V.

II. Proposed Observer

Consider a nonlinear system represented by the equations

$$\dot{z}(t) = f(z(t), x(t)) \tag{1}$$

$$y(t) = Cz(t) \tag{2}$$

where $z(t) \in R^q$ is the state, $x(t) \in R^p$ the input, $y(t) \in R^m$ the output, and C a $m \times q$ matrix. The function $f(\cdot,\cdot)$ and the input $x(\cdot)$ are assumed to be C^1-functions. For the sake of simplicity we are restricted to linear time-invariant readout maps. The important case where some of the state variables can be measured directly is thereby treated. Furthermore, the linear time-invariant readout map is well suited to pointing out the main idea. Some remarks on the more general case with nonlinear readout maps are given in Section III. For the considerations following below we need a slightly more general definition of the exponential observer in [8].

Definition: For a dynamic system given by (1) and (2) an exponential observer is a dynamic system

$$\dot{\hat{z}}(t) = f(\hat{z}(t), x(t)) + g(y(t), \hat{z}(\cdot), x(\cdot), t) \tag{3}$$

with an output injection $g(\cdot,\cdot,\cdot,\cdot)$ such that

$$\|z(t) - \hat{z}(t)\| \le \eta \|z(0) - \hat{z}(0)\| e^{-\theta t} \qquad \forall t \ge 0, \quad \forall z(0) - \hat{z}(0) \in B_\rho \tag{4}$$

holds for some $\rho, \eta, \theta \in R^+$ with $B_\rho = \{v \in R^q : \|v\| < \rho\}$.

Remark: The output injection $g(\cdot,\cdot,\cdot,\cdot)$ depends in general on the whole functions $\hat{z}(\cdot)$ and $x(\cdot)$ and not only on the recent values $\hat{z}(t)$ and $x(t)$. The reasons are given below.

To calculate the output injection $g(\cdot,\cdot,\cdot,\cdot)$ we introduce a Riccati differential equation which is similar to the Riccati differential equation for the extended Kalman filter [5]. Using the abbreviation

$$A(t) = \frac{\partial f}{\partial z}(\hat{z}(t), x(t)) \tag{5}$$

it reads

$$\dot{P}(t) = A(t)P(t) + P(t)A^T(t) - P(t)(C^T R^{-1} C - \lambda^2 I)P(t) + \mu^2 I \tag{6}$$

with some $\lambda, \mu \in R^+$ and a positive definite symmetric matrix R. We define the observer gain by

$$K(t) = P(t)C^T R^{-1} \tag{7}$$

and the output injection by

$$g(y(t), \hat{z}(\cdot), x(\cdot), t) = K(t)(y(t) - C\hat{z}(t)). \tag{8}$$

It is necessary to allow a general dependence on $\hat{z}(\cdot)$ and $x(\cdot)$ and not only on the recent values $\hat{z}(t)$ and $x(t)$ because the solution

Manuscript received March 25, 1996; revised September 23, 1996 and March 18, 1997. This work was supported in part by the Universität Erlangen-Nürnberg and by the Flughafen Frankfurt Main Stiftung.

K. Reif is with the BMW AG, 80788 Munich, Germany (e-mail: konrad.reif@mailexcite.com).

F. Sonnemann is with the Diehl GmbH, Nürnberg, Germany.

R. Unbehauen is with the Lehrstuhl für Allgemeine und Theoretische Elektrotechnik, Universität Erlangen-Nürnberg, 91058 Erlangen, Germany.

Publisher Item Identifier S 0018-9286(99)00669-8.

of the Riccati differential equation (6) depends on past values of $A(t) = (\partial f/\partial z)(\hat{z}(t), x(t))$.

An expansion of $f(\cdot,\cdot)$ at $\hat{z}(t)$, $x(t)$ leads to

$$\begin{aligned} &f(z(t),x(t)) - f(\hat{z}(t),x(t)) \\ &\quad = A(t)(z(t)-\hat{z}(t)) + \varphi(z(t),\hat{z}(t),x(t)) \end{aligned} \tag{9}$$

where $\varphi(z(t),\hat{z}(t),x(t))$ are the terms of second- and higher order in $z(t)-\hat{z}(t)$. Defining the estimation error by

$$\zeta(t) = z(t) - \hat{z}(t) \tag{10}$$

subtracting (3) from (1) and considering (8) and (9), we obtain

$$\dot{\zeta}(t) = (A(t) - K(t)C)\zeta(t) + \varphi(z(t),\hat{z}(t),x(t)). \tag{11}$$

For an exponential observer this differential equation has an exponentially stable equilibrium point at zero; moreover, if (4) holds for all $\zeta(0) \in R^q$ the equilibrium point is globally exponentially stable (cf. [21, Sec. 5.1, p. 143]).

To state the proof of the Main theorem given below we need the following preparation.

Lemma: Consider real vectors $z, \hat{z} \in R^q$ and $x \in R^p$, a symmetric $q \times q$ matrix Π, and a function $\varphi(\cdot,\cdot,\cdot)$ with

$$\|\varphi(z,\hat{z},x)\| \le \kappa\|z-\hat{z}\| \tag{12}$$

for some $\kappa \in R^+$. Choose $\lambda, \mu \in R^+$ such that $\kappa < \lambda\mu$ holds. Then there is a $\delta > 0$ such that

$$2(z-\hat{z})^T\Pi\varphi(z,\hat{z},x) \le (z-\hat{z})^T\left[\lambda^2 I + (\mu^2-\delta)\Pi\Pi\right](z-\hat{z}) \tag{13}$$

holds.

Proof: From $\kappa < \lambda\mu$ it follows that there is a $0 < \delta' < \lambda\mu$ such that

$$\kappa < \lambda\mu - \delta'$$

holds. Inserting into (12) yields

$$\|\varphi(z,\hat{z},x)\| \le (\lambda\mu - \delta')\|z-\hat{z}\|$$

and therefore we have

$$2(z-\hat{z})^T\Pi\varphi(z,\hat{z},x) \le 2(\lambda\mu-\delta')\|\Pi(z-\hat{z})\|\|z-\hat{z}\|. \tag{14}$$

For considerations following below we evaluate the square

$$\begin{aligned} &\left(\left(\mu - \frac{\delta'}{\lambda}\right)\|\Pi(z-\hat{z})\| - \lambda\|z-\hat{z}\|\right)^2 \\ &= \left(\mu^2 - \frac{2\mu\delta'}{\lambda} + \frac{\delta'^2}{\lambda^2}\right)(z-\hat{z})^T\Pi\Pi(z-\hat{z}) \\ &\quad - 2\lambda\left(\mu - \frac{\delta'}{\lambda}\right)\|\Pi(z-\hat{z})\|\|z-\hat{z}\| + \lambda^2(z-\hat{z})^T(z-\hat{z}) \ge 0 \end{aligned}$$

and use the fact that it takes only nonnegative values. Rearranging the terms yields

$$\begin{aligned} &2(\lambda\mu-\delta')\|\Pi(z-\hat{z})\|\|(z-\hat{z})\| \\ &\quad \le (z-\hat{z})^T\left[\left(\mu^2 - \left(\frac{2\mu\delta'}{\lambda} - \frac{\delta'^2}{\lambda^2}\right)\right)\Pi\Pi + \lambda^2 I\right](z-\hat{z}). \end{aligned} \tag{15}$$

Choosing

$$\delta = \frac{2\mu\delta'}{\lambda} - \frac{\delta'^2}{\lambda^2}$$

from $\delta' < \lambda\mu$ it follows that $\mu > \delta'/\lambda$ and therefore

$$\delta > 2\frac{\delta'}{\lambda}\frac{\delta'}{\lambda} - \frac{\delta'^2}{\lambda^2} > 0.$$

Combining (14) and (15) we obtain the desired result (13). □

With these preliminaries we are able to state Theorem 1.

Theorem 1: Consider a nonlinear system with linear time-invariant readout map given by (1), (2) and an observer given by (3) and (6)–(8) with some $\lambda, \mu > 0$ and a positive definite matrix R, such that the following conditions hold.

1) For any solution $\hat{z}(\cdot)$ of the observer differential equation (3) the solution $P(\cdot)$ of the Riccati differential equation (6) is bounded via
$$\underline{p}I \le P(t) \le \bar{p}I \tag{16}$$
for some $\underline{p}, \bar{p} > 0$.
2) The nonlinear terms $\varphi(z(t),\hat{z}(t),x(t))$ in the differential equation (11) for the estimation error are bounded via
$$\|\varphi(z(t),\hat{z}(t),x(t))\| \le \kappa\|z(t)-\hat{z}(t)\| \tag{17}$$
with $\kappa < \lambda\mu$.

Then the considered observer is an exponential observer. Moreover, the differential equation (11) for the estimation error is globally exponentially stable at zero.

Remarks:

1) To ensure the global exponential stability of the differential equation (11) we require that (17) is satisfied in the whole state space. If this inequality holds only in a restricted area, only local exponential stability can be guaranteed. This means that in this case the initial estimation error may not be arbitrary large. Nevertheless, numerical simulations have shown that even if the stability is not globally satisfied, the proposed observer can tolerate much higher initial estimation errors than an observer based on the extended Kalman filter (see Section IV).
2) Using similar techniques as in the proof following below, it can be shown that under certain conditions the continuous-time extended Kalman filter is an exponential observer [16], [18] too. The difference is that the equilibrium point of the estimation error is globally exponentially stable for the proposed observer but not for the extended Kalman filter. This means that the proposed observer can tolerate arbitrary large initial estimation errors, which is not the case for the extended Kalman filter.
3) For the usual extended Kalman filter it can be shown that the solution of the Riccati differential equation is bounded via (16), if the matrices $A(t)$ and C fulfill the uniform observability condition [7] or if the nonlinear system satisfies a certain detectability condition as stated in [1]. Unfortunately, these conditions cannot be applied to get similar results for the H_∞-filtering-like Riccati differential equation (6). (The reason is that the term $C^TR^{-1}C - \lambda^2 I$ is in general not positive definite because $C^TR^{-1}C$ does not have full rank if we treat nontrivial observation problems.) It is a well-known problem arising in H_∞-control as well as H_∞-filtering that the solutions of the corresponding algebraic Riccati equations and Riccati differential equations may lack being positive definite (cf. [3]).
4) For the proof below as well as for the lemma stated above, the parameter μ does not play any important role. It has been introduced to have an additional degree of freedom during the implementation process. Especially for ensuring Condition 1, the additional design parameter μ has turned out to be very useful. Also see the following remark.
5) The existence of a solution $P(\cdot)$ for the Riccati differential equation (6) which satisfies Condition 1 depends mainly on an

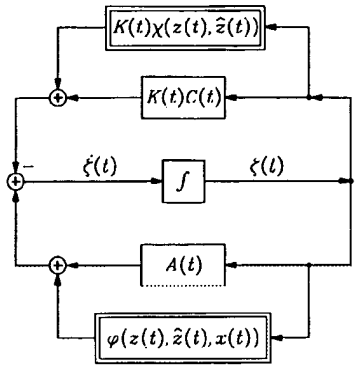

Fig. 1. Block diagram corresponding to the differential equation (27).

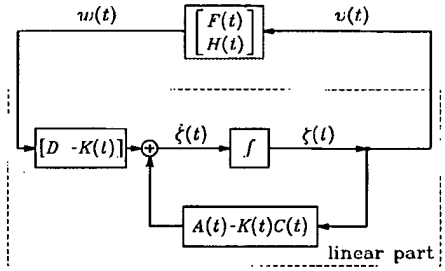

Fig. 2. Block diagram corresponding to the differential equation (31). The whole system consists of two interconnected subsystems. The dashed box contains the linear part of the system and the observer; $F(t)$ and $H(t)$ represent the higher order nonlinear terms.

appropriate choice of λ and μ. As will be shown in Section III, they are closely related to the attenuation constant γ in H_∞-filtering problems. To find suitable values for λ and μ we employed a binary search algorithm, which is widely used to solve H_∞-control and H_∞-filtering problems (see, e.g., [3]) and adapted it for our purpose (see Section IV).

Proof: We consider the differential equation (11) for the estimation error and prove its exponential stability by choosing the Lyapunov function

$$V(\zeta(t),t) = \zeta^T(t)\Pi(t)\zeta(t) \tag{18}$$

with $\Pi(t) = P^{-1}(t)$. Because of Assumption 1 we have the following bounds for the Lyapunov function:

$$\frac{1}{\bar{p}}\|\zeta(t)\|^2 \le V(\zeta(t),t) \le \frac{1}{\underline{p}}\|\zeta(t)\|^2 \tag{19}$$

which imply positive definiteness and decrescence. The time derivative of the Lyapunov function reads

$$\dot{V}(\zeta(t),t) = \dot{\zeta}^T(t)\Pi(t)\zeta(t) + \zeta^T(t)\dot{\Pi}(t)\zeta(t) + \zeta^T(t)\Pi(t)\dot{\zeta}(t).$$

Inserting $\dot{\zeta}(t)$ according to the differential equation (11) yields

$$\begin{aligned}\dot{V}(\zeta(t),t) = {} & \zeta^T(t)\dot{\Pi}(t)\zeta(t) + [(A(t) - K(t)C)\zeta(t) \\ & + \varphi(z(t),\hat{z}(t),x(t))]^T\Pi(t)\zeta(t) \\ & + \zeta^T(t)\Pi(t)[(A(t) - K(t)C)\zeta(t) + \varphi(z(t),\hat{z}(t),x(t))].\end{aligned}$$

Applying the lemma and considering (7) we get with $\kappa < \lambda\mu$

$$\begin{aligned}\dot{V}(\zeta(t),t) \le {} & \zeta^T(t)[\dot{\Pi}(t) + \Pi(t)A(t) + A^T(t)\Pi(t) \\ & - 2C^TR^{-1}C + (\mu^2 - \delta)\Pi(t)\Pi(t) + \lambda^2 I]\zeta(t).\end{aligned}$$

Using

$$\dot{\Pi}(t) = -\Pi(t)\dot{P}(t)\Pi(t) \tag{20}$$

and the Riccati differential equation (6) leads to

$$\dot{V}(\zeta(t),t) \le \zeta^T(t)[-\delta\Pi(t)\Pi(t) - C^TR^{-1}C]\zeta(t). \tag{21}$$

With the bounds (16) for $P(t)$ we obtain the inequality

$$\dot{V}(\zeta(t),t) \le -\frac{\delta}{\bar{p}^2}\|\zeta(t)\|^2 \tag{22}$$

which implies that the time derivative of the Lyapunov function is negative definite. With (19) and (22) we satisfy the requirements to apply [21, Th. 62, Sec. 5.3, p. 173] and conclude that the differential equation (11) has a globally exponentially stable equilibrium point at zero. This includes that the considered observer is an exponential observer. □

III. Relations to H_∞-Filtering and Robust Control Theory

Considering the small gain theorem the proposed observer is closely related to H_∞-filtering theory as will be shown below. Since these relations are more obvious for the case with nonlinear readout maps, we let a nonlinear continuous-time system be given by

$$\dot{z}(t) = f(z(t),x(t)) \tag{23}$$

$$y(t) = h(z(t)) \tag{24}$$

with a C^1-function $h(\cdot)$. The linear readout map is thereby contained as a special case. For this nonlinear system we construct an observer according to (3) and (6)–(8). Using the fact that the functions $f(\cdot,\cdot)$ and $h(\cdot)$ are continuously differentiable, we expand them via (9) and

$$h(z(t)) - h(\hat{z}(t)) = C(t)(z(t) - \hat{z}(t)) + \chi(z(t),\hat{z}(t)) \tag{25}$$

where $C(t)$ is an $m \times q$ matrix given by

$$C(t) = \frac{\partial h}{\partial z}(\hat{z}(t)). \tag{26}$$

Defining the estimation error by (10) we obtain from (23) and (3) using (8), (9), and (25)

$$\begin{aligned}\dot{\zeta}(t) = {} & (A(t) - K(t)C(t))\zeta(t) + \varphi(z(t),\hat{z}(t),x(t)) \\ & - K(t)\chi(z(t),\hat{z}(t)).\end{aligned} \tag{27}$$

The nonlinear terms are assumed to satisfy (17) as well as

$$\|\chi(z(t),\hat{z}(t))\| \le \lambda\|z(t) - \hat{z}(t)\| \tag{28}$$

with some $\lambda > 0$. Now we have a closer look at the differential equation (27) for the estimation error. Fig. 1 shows the corresponding block diagram. Defining

$$F(t) = \frac{1}{\mu\|\zeta(t)\|^2}\varphi(z(t),\hat{z}(t),x(t))\zeta^T(t) \tag{29}$$

$$H(t) = \frac{1}{\|\zeta(t)\|^2}\chi(z(t),\hat{z}(t))\zeta^T(t) \tag{30}$$

for $\zeta(t) \neq 0$ we have from (27)

$$\dot{\zeta}(t) = (A(t) - K(t)C(t) + DF(t) - K(t)H(t))\zeta(t) \tag{31}$$

with $D = \mu I$ as shown in Fig. 2. Moreover, we obtain

$$\left\|\begin{bmatrix}F(t)\\H(t)\end{bmatrix}\right\| < \lambda$$

for every $t \ge 0$ which is an immediate consequence of (17), (28)–(30), and $\kappa < \lambda\mu$. By this construction the nonlinearities are considered as time-varying uncertainties. For the stability of (31), we have the following theorem.

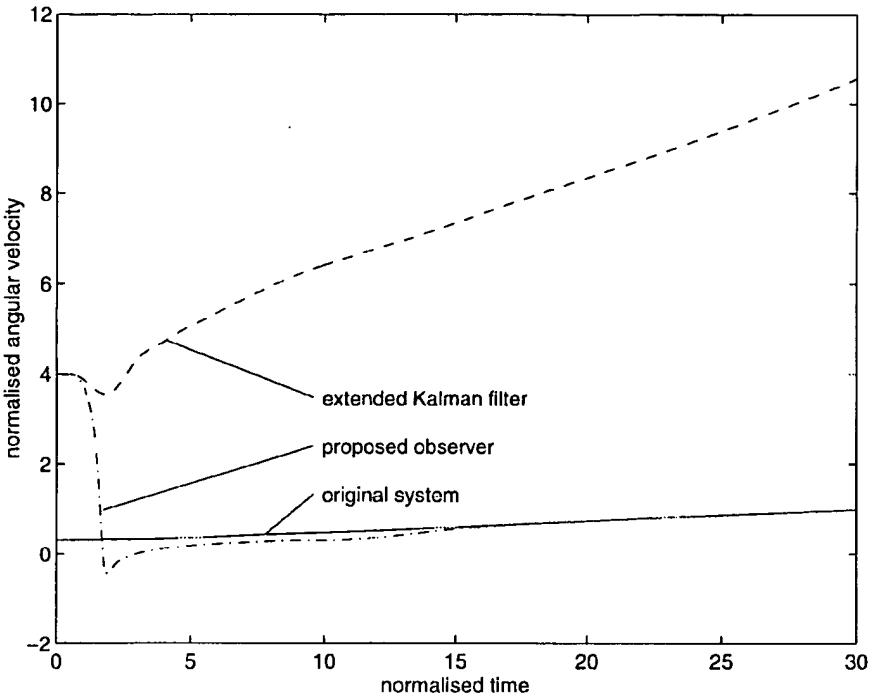

Fig. 3. Normalized angular velocity $z_5(t)$ for the original system, the proposed observer, and the extended Kalman filter with a medium initial estimation error.

Theorem 2: Consider (31) with $D = \mu I$ and an observer gain $K(t)$ given by (6) and (7) with $\lambda, \mu > 0$, and $R = I$. Let the following conditions hold.

1) The Riccati differential equation (6) has a solution $P(\cdot)$ which is bounded via

$$\underline{p} I \leq P(t) \leq \bar{p} I$$

for some $\underline{p}, \bar{p} > 0$.

2) The matrices $F(t)$ and $H(t)$ are norm-bounded by

$$\left\| \begin{bmatrix} F(t) \\ H(t) \end{bmatrix} \right\| < \lambda$$

for every $t \geq 0$.

Then the system (31) is exponentially stable.

Proof: For the proof of this theorem we employ a variant of the small gain theorem. We recall the operator norms [10] for the two subsystems in Fig. 2 (e.g., $[F^T(t)\ H^T(t)]^T$ and the part inside the dashed box)

$$\|T_{wv}\|_\infty = \sup_{\substack{w \in L_2 \\ \|w\|_2 \neq 0}} \frac{\|w\|_2}{\|v\|_2}, \qquad \|T_{vw}\|_\infty = \sup_{\substack{v \in L_2 \\ \|v\|_2 \neq 0}} \frac{\|v\|_2}{\|w\|_2}$$

where $\|\cdot\|_2$ denotes the usual L_2-norm for functions. According to [20, Corollary 1], the whole system in Fig. 2 is exponentially stable if the subsystem in the dashed box is exponentially stable and the small gain condition

$$\|T_{vw}\|_\infty \|T_{wv}\|_\infty < 1 \tag{32}$$

is satisfied. The operator norm $\|T_{wv}\|_\infty$ can be estimated easily to

$$\|T_{wv}\|_\infty = \sup_{t \geq 0} \left\| \begin{bmatrix} F(t) \\ H(t) \end{bmatrix} \right\| < \lambda. \tag{33}$$

Moreover, it can be seen that the subsystem inside the dashed box in Fig. 2 has the structure of a H_∞-filter. Introducing $\gamma = 1/\lambda$ and using $R = I$, $D = \mu I$ the Riccati differential equation (6) can be rewritten in the form

$$\dot{P}(t) = A(t)P(t) + P(t)A^T(t) - P(t)C^T(t)C(t)P(t) + \frac{P(t)P(t)}{\gamma^2} + DD^T \tag{34}$$

and the observer gain (7) is given by

$$K(t) = P(t)C^T(t). \tag{35}$$

With (34) and (35) we are able to employ standard results in H_∞-filtering (cf. [2, Sec. 7.4, p. 301, Th. 7.6] or [6, Sec. 7.2.2, p. 267, Th. 7.2.1]) and conclude that the subsystem inside the dashed box in Fig. 2 is exponentially stable and the operator norm $\|T_{vw}\|_\infty$ is bounded by

$$\|T_{vw}\|_\infty \leq \gamma.$$

Together with (33) and $\gamma = 1/\lambda$ we fulfill the small gain condition (32) and the proof is completed. □

IV. Application to an Example System

To examine the practical usefulness of the proposed observer we apply it to a highly nonlinear example system, a symmetrical three-phase induction motor. The quantities to be estimated are the rotor flux and the angular velocity (see also [19] and the references cited therein). We introduce the state differential equations for an induction machine and do not mention too many details about the physical meanings of the considered quantities, which are contained in any standard book about electrical drives (see, e.g., [12, Sec. 10.1] or [15, Sec. 3.3]). The state differential equations of a symmetrical three-phase induction machine read

$$\dot{z}_1(t) = k_1 z_1(t) + x_1(t) z_2(t) + k_2 z_3(t) + x_2(t) \tag{36}$$

$$\dot{z}_2(t) = -x_1(t) z_1(t) + k_1 z_2(t) + k_2 z_4(t) \tag{37}$$

$$\dot{z}_3(t) = k_3 z_1(t) + k_4 z_3(t) + (x_1(t) - z_5(t)) z_4(t) \tag{38}$$

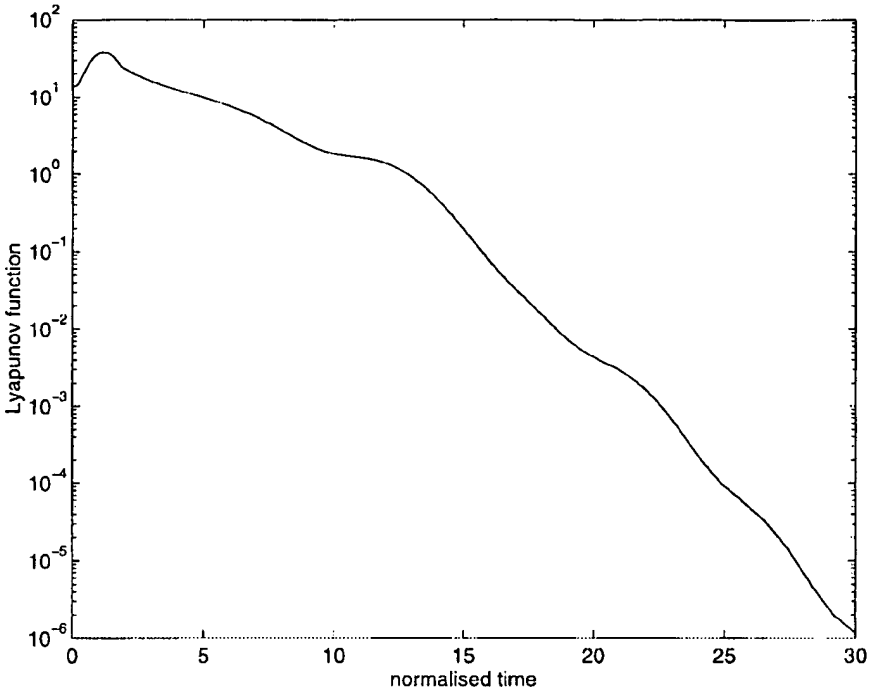

Fig. 4. Lyapunov function $V(\zeta(t), t)$ for the proposed observer.

$$\dot{z}_4(t) = k_3 z_2(t) - (x_1(t) - z_5(t))z_3(t) + k_4 z_4(t) \quad (39)$$

$$\dot{z}_5(t) = k_5(z_1(t)z_4(t) - z_2(t)z_3(t)) + k_6 x_3(t). \quad (40)$$

All state variables are normalized. $z_1(t)$, $z_2(t)$ and $z_3(t)$, $z_4(t)$ are the components of the stator and the rotor flux, respectively, in the plane perpendicular to the rotation axis. $z_5(t)$ is the angular velocity, $x_1(t)$ the frequency, and $x_2(t)$ the amplitude of the stator voltage, respectively, and $x_3(t)$ is the torque of the load. $k_1, \cdots, k_6$ are several parameters depending on the considered drive.

The output are the normalized stator currents $y_1(t)$ and $y_2(t)$, leading to the output equations

$$y_1(t) = k_7 z_1(t) + k_8 z_3(t) \quad (41)$$

$$y_2(t) = k_7 z_2(t) + k_8 z_4(t) \quad (42)$$

with parameters k_7 and k_8. The matrix $A(t)$ can be calculated from (36)–(40), parameter t omitted

$$A(t) = \begin{bmatrix} k_1 & x_1 & k_2 & 0 & 0 \\ -x_1 & k_1 & 0 & k_2 & 0 \\ k_3 & 0 & k_4 & x_1 - \hat{z}_5 & -\hat{z}_4 \\ 0 & k_3 & \hat{z}_5 - x_1 & k_4 & \hat{z}_3 \\ k_5\hat{z}_4 & -k_5\hat{z}_3 & -k_5\hat{z}_2 & k_5\hat{z}_1 & 0 \end{bmatrix} \quad (43)$$

and the output matrix is given by (41), (42)

$$C = \begin{bmatrix} k_7 & 0 & k_8 & 0 & 0 \\ 0 & k_7 & 0 & k_8 & 0 \end{bmatrix}. \quad (44)$$

For the simulation we set $k_1 = -0.186$, $k_2 = 0.178$, $k_3 = 0.225$, $k_4 = -0.234$, $k_5 = -0.081$, $k_6 = -0.018$, $k_7 = 4.643$, $k_8 = -4.448$, $x_1(t) = s(t)$, $x_2(t) = s(t)$, and $x_3(t) = 0$, where $s(t)$ is the unit step function. These values are obtained, if in the original unnormalized system certain values for the physical quantities are chosen. To obtain appropriate values for λ and μ we propose a binary search algorithm consisting of the following steps.

1) Choose $\lambda, \mu > 0$ and $R = rI$ with some $r > 0$.
2) Decrease r by taking the half-value until the solution $P(\cdot)$ of the Riccati differential equation (6) takes positive definite values. If no positive definite solution can be achieved, proceed with Step 3).
3) Decrease μ by taking the half-value and initialize $R = rI$ as in Step 1). Proceed with Step 2). If μ gets smaller than a prescribed bound μ_0 we let the algorithm abort.

For the simulations we insert $A(t)$ and C into the Riccati differential equation (6) and choose $\lambda^2 = 0.7$, $\mu^2 = 0.008$, and $R = 0.06I$ according to the above stated search algorithm. The observer gain is given by (7) and the differential equation for the observer by (3) and (8). We solved the state differential equations numerically by the Runge–Kutta method choosing the initial conditions

$$z(0) = [0.2 \quad -0.6 \quad -0.4 \quad 0.1 \quad 0.3]^T \quad (45)$$

for the system to be observed and

$$\hat{z}(0) = [0.5 \quad 0.1 \quad 0.3 \quad -0.2 \quad 4]^T \quad (46)$$

for the observer. For the sake of comparison we also computed a usual extended Kalman filter [5] with the same weighting matrices $\mu^2 I$, R and the same initial condition $\hat{z}(0)$ by setting $\lambda = 0$, $\mu^2 = 0.008$, and $R = 0.06I$ in (6).

Figs. 3 and 4 show the simulation results. As shown in Fig. 3 the estimation error approaches zero for the proposed observer but not for the extended Kalman filter. Further simulation results have shown that the proposed observer has often a larger domain of attraction than the extended Kalman filter, i.e., the initial estimation error may be larger. The Lyapunov-function (18) is depicted in Fig. 4. Looking at the values for $0 \leq t \leq 1$ we see that the Lyapunov function is increasing. This means that (22) is sufficient but not necessary for the error decay.

V. Conclusion

The purpose of this paper is to propose an observer for nonlinear systems. This is done by modifying the well-known extended Kalman filter [5] for an effective treatment of the nonlinearities. We proved that under certain conditions this observer is an exponential observer [8] by choosing an appropriate Lyapunov function. For an alternative approach to the proposed observer we consider the nonlinearities as uncertainties and get a stabilization problem which is typical in robust control theory [9], [20]. This stabilization problem can be solved by H_∞-filtering techniques [2], [6], [10], [14] leading to the proposed modification of the extended Kalman filter. Using the proposed observer to estimate the rotor flux and the angular velocity of an induction motor we show that it can be easily applied to complex highly nonlinear systems. Numerical simulations show a good performance and an increased domain of convergence in comparison to the extended Kalman filter, i.e., we can tolerate larger initial estimation errors. Similar to H_∞-filtering problems, we have in general not a bounded positive definite solution of the corresponding Riccati differential equation, which does exist for the extended Kalman filter if the system satisfies certain observability conditions [1]. Therefore, a careful choice of the constants in this Riccati differential equation is of particular interest.

Acknowledgment

The authors would like to thank T. Katayama and the anonymous referees for their insightful comments.

References

[1] J. Baras, A. Bensoussan, and M. R. James, "Dynamic observers as asymptotic limits of recursive filters: Special cases," *SIAM J. Appl. Math.*, vol. 48, pp. 1147–1158, 1988.
[2] T. Basar and B. Bernhard, *H_∞-Optimal Control and Related Minimax Design Problems*. Boston, MA: Birkhäuser, 1995.
[3] R. Y. Chiang and M. G. Safonov, *Robust Control Toolbox User's Guide*. Natick, MA: The Mathworks, 1992.
[4] J. C. Doyle, B. A. Francis, and A. R. Tannenbaum, *Feedback Control Theory*. New York: Macmillan, 1992.
[5] A. Gelb, *Applied Optimal Estimation*. Cambridge, MA: MIT Press, 1984.
[6] M. Green and D. J. N. Limebeer, *Linear Robust Control*. Englewood Cliffs, NJ: Prentice-Hall, 1995.
[7] R. E. Kalman, "New methods in Wiener filtering theory," in *Proc. 1st Symp. on Eng. Appl. of Random Function Theory and Probability*, J. Bogdanoff and F. Kozin, Eds. New York: Wiley, 1963, pp. 270–388.
[8] S. R. Kou, D. L. Elliott, and T. J. Tarn, "Exponential observers for nonlinear dynamic systems," *Inform. Contr.*, vol. 29, pp. 204–216, 1975.
[9] P. P. Khargonekar, I. R. Petersen, and K. Zhou, "Robust stabilization of uncertain linear systems: Quadratic stabilizability and H_∞ control theory," *IEEE Trans. Automat. Contr.*, vol. 35, pp. 356–361, 1990.
[10] P. P. Khargonekar, "State space H_∞ control theory and the LQG problem," in *Mathematical System Theory*, A. Antoulas, Ed. 1991, pp. 159–176.
[11] H. Kwakernaak, "Robust control and H_∞-optimization," *Automatica*, vol. 29, pp. 255–273, 1993.
[12] W. Leonhard, *Control of Electrical Drives*. Berlin, Germany: Springer-Verlag, 1985.
[13] E. A. Misawa and J. K. Hedrick, "Nonlinear observers—A state-of-the-art survey," *ASME J. Dyn. Syst. Meas. Contr.*, vol. 111, pp. 344–352, 1989.
[14] K. M. Nagpal and P. P. Khargonekar, "Filtering and smoothing in a H_∞-setting," *IEEE Trans. Automat. Contr.*, vol. 36, pp. 152–166, 1991.
[15] G. Pfaff, *Regelung Elektrischer Antriebe I*. München, Germany: Oldenbourg Verlag, 1990.
[16] K. Reif and R. Unbehauen, "Linearization along trajectories and the extended Kalman filter," in *Proc. 13th IFAC World Congr.*, 1996, vol. H, pp. 509–514.
[17] K. Reif, F. Sonnemann, and R. Unbehauen, "Modification of the extended Kalman filter with an additive term of instability," in *Proc. 35th IEEE Conf. Decision and Control*, Kobe, Japan, 1996, pp. 4058–4059.
[18] K. Reif, "Steuerung von nichtlinearen systemen mit Homotopie-Verfahren," *Fortschritt-Berichte VDI*, vol. 8. Düsseldorf, Germany: VDI-Verlag, 1997.
[19] L. Salvatore, S. Stasi, and L. Tarchioni, "A new EKF-based algorithm for flux estimation in induction machines," *IEEE Trans. Ind. Electron.*, vol. 40, pp. 496–504, 1993.
[20] G. Tadmor, "Uncertain feedback loops and robustness in general linear systems," *Automatica*, vol. 27, pp. 1039–1042, 1991.
[21] M. Vidyasagar, *Nonlinear Systems Analysis*. Englewood Cliffs, NJ: Prentice-Hall, 1993.
[22] B. L. Walcott, M. J. Corless, and S. H. Zak, "Comparative study of nonlinear state-observation techniques," *Int. J. Contr.*, vol. 45, pp. 2109–2132, 1987.

Fractional-Order Systems and $PI^\lambda D^\mu$-Controllers

Igor Podlubny

***Abstract*— Dynamic systems of an arbitrary real order (fractional-order systems) are considered. A concept of a fractional-order $PI^\lambda D^\mu$-controller, involving fractional-order integrator and fractional-order differentiator, is proposed. The Laplace transform formula for a new function of the Mittag–Leffler-type made it possible to obtain explicit analytical expressions for the unit-step and unit-impulse response of a linear fractional-order system with fractional-order controller both for the open and closed loop. An example demonstrating the use of the obtained formulas and the advantages of the proposed $PI^\lambda D^\mu$-controllers is given.**

***Index Terms*— Fractional-order controllers, fractional-order systems, fractional differential equations, Laplace transforms, transfer functions.**

I. Introduction

Recently, several authors have considered mechanical systems described by fractional-order state equations [4], [5], [15], which means equations involving so-called fractional derivatives and integrals (for the introduction to this theory see [21]).

There are also several recent applications in electricity.

Le Méhauté and Crepy [14] have proposed a concept of a *fractance*—a new electrical circuit element, which has intermediate properties between resistance and capacitance. Such a device has been experimentally studied, for example, by Nakagawa and Sorimachi [18]. A circuit proposed by Oldham and Zoski [22] provides another example of a fractance.

A new capacitor theory developed by Westerlund [28] is based on the use of fractional derivatives.

New fractional derivative-based models are more adequate than the previously used integer-order models. This has been demonstrated, for instance, by Caputo [7], Nonnenmacher and Glöckle [19], Friedrich

Manuscript received August 29, 1997.

The author is with the Department of Management and Control Engineering, B.E.R.G. Faculty, Technical University of Kosice, 04200 Kosice, Slovak Republic (e-mail: podlbn@ccsun.tuke.sk).

Publisher Item Identifier S 0018-9286(99)00671-6.

Info about this **Ph.D. DISSERTATION**

Title	"Optimum Vibration Control of Distributed Parameter Rotor Bearing System by Using Electromagnetic Bearing"
Author	Kim, J.S.
Graduation	August 1989
Note	Associate Professor, Hankuk Aviation University
Abstract	As the modern rotor systems have a tendency of being operated at high speed and designed to be lighter, the control of excessive vibration becomes more and more important because of increasing requirement in accuracy and reliability. Since the flexible rotor bearing system is a typical hyperbolic type distributed parameter system, the control, passive or active, not accounting for such a nature often does not yield satisfactory performance. The primary objective of this study is to develop efficient control design methods which account for and use the distributed parameter and isotropic properties. The output feedback control scheme accounts for the practical aspects such as the observation and related stability problems caused by spillover effects, while the optimal design deals mainly with the theoretical and numerical aspects. Optimal pole assignment in distributed parameter control systems is established and the existence of optimal solution is proven in case of compact linear feedback. The method, an extension of the finite dimensional design, gives the solution of the operator Riccati equation which is known to be one of the most difficult problems faced by the designers. By adopting the complex notation for the isotropic systems, it is shown that the closed loop eigenstructure is determined, contrary to the real field design, so as to preserve the isotropic property. In order to utilize the xymmetric property between the two directional vibrations: vertical and horizontal or forward and backward, a new control scheme is designed by introducing the complex state for the systems having the isotropic property. The algebraic relations concerning distribution of the eigenvalues of complex matrices are developed so as to cluster the poles into specified regions, rather than fixed positions, imposing the relative stability margin, e.g., uniform damping or uniform damping ratio. The closed loop eigenstructure has the direct one-to-one relation with the physical parameters and the isotropic property is preserved under feedback control. The method transforms Riccati equation to Lyapunov equation of the same dimension so that computational effort is almost removed. It is shown that the method can be used effectively in vibration control of rotating machinery such as the isotropic rotor bearing system, the magnetic bearing system and the rotating circular disk. To achieve the dual objective of stabilization and spillover suppression, a constrained output feedback control scheme is developed based on the optimization of a modified performance index which includes spillover terms. In order to construct the appropriate performance index, the method makes use of the two-time scale property of the primary and secondary modes. The control model is constructed based on the singularly perturbed modal model, which retains the simple modal structure while preserving the accuracy of the frequency domain modeling. A set of optimality condition is derived and iterative solution procedure is also presented. A set of simulation examples show the effectiveness of the proposed scheme. In order to control the rotation related periodic disturbances, a disturbance accommodating controller is also designed based on the disturbance estimator. The main advantage of the proposed scheme is the simplicity in numerical calculation and estimator structures, requiring only a solution of non-symmetric Lyapunov equation of relatively small order. Lyapunov equation is the first order perturbation solution of the matrix cubic equation which yields the exact solution. Through the matrix perturbation analysis, it is proven that, for small gain, the approximate solution converges to the exact one. The control scheme is proven to effectively control the build up vibration subject to sudden imbalance through the numerical simulational. Finally, the output feedback control experiment is performed by using a magnetic bearing when the rotor system is subject to external impulse and imbalance. The magnetic bearing with four magnets is manufactured and the analog design is transformed to the discretized form and implemented by using a 16 bit microcomputer. The control model is constructed by using the experimentally obtained modal parameters through a set of modal testings in complex coordinates. The proposed control scheme enables the rotor to run through the first critical speed without excessive vibration against the initial system unbalance. In order to verify the performance of the proposed control

initial system unbalance. In order to verify the performance of the proposed control scheme, the results are compared with the numerical ones. It is shown that the experimental results are fairly well coincident with the predicted ones. In conclusion, through the extensive analysis and experiments, it is shown that the proposed controllers can be used effectively in practical implementation as well as in theoretical and numerical aspect of controller design for the rotor bearing systems.

Development of a servowriter for magnetic disk storage applications

Brown, D.H. Sri-Jayantha, M.
IBM Applications Bus. Syst., Rochester, MN, USA;

This paper appears in: **Instrumentation and Measurement, IEEE Transactions on**

Publication Date: April 1990
On page(s): 409 - 415
Volume: 39 , Issue: 2
ISSN: 0018-9456
Reference Cited: 7
CODEN: IEIMAO
Inspec Accession Number: 3680870

Abstract:
The design, development, and application of a research servowriter, which is necessary to record magnetic position encoding schemes, are presented. The servowriter is designed to evaluate emerging disk drive technologies. Submicron positioning accuracy of the disk actuator is achieved by integrating the **state**-of-the-art electronic, optic, electromechanical, and digital signal processing hardware. The servowriter also provides flexible and sophisticated signal encoding schemes through a programmable pattern generator and has several modules of customized electronic hardware, each controlled by a supervisory computer. The position of the R/W (read/write) head and actuator assembly is measured by a laser interferometric system. The measured position is used to estimate the velocity of the R/W head, which is then used to implement a **state**-variable-based proportional-integral-derivative controller on the Intel (8086/8087) microprocessor chip set. Both systematic and random error sources associated with phase and amplitude encoding schemes are described. Environmental factors such as seismic **vibration** and temperature change, which indirectly contribute to servowriting errors, are identified, and steps to contain these error sources are described

Index Terms:
computerised control encoding laser beam applications light interferometry magnetic **disc** storage microcomputer applications position control servomechanisms three-term control velocity control Intel amplitude encoding disk drive error laser interferometric system magnetic disk storage magnetic position encoding microprocessor chip modules phase encoding

programmable pattern generator seismic **vibration** servowriter **state**-variable-based proportional-integral-derivative controller submicron positioning temperature velocity

Documents that cite this document
There are no citing documents available in IEEE Xplore at this time.

Search Results [PDF FULL-TEXT 644 KB] PREV NEXT DOWNLOAD CITATION

Home | Log-out | Journals | Conference Proceedings | Standards | Search by Author | Basic Search | Advanced Search | Join IEEE | Web Account | New this week | OPAC Linking Information | Your Feedback | Technical Support | Email Alerting | No Robots Please | Release Notes | IEEE Online Publications | Help | FAQ| Terms | Back to Top

Development of a Servowriter for Magnetic Disk Storage Applications

DANA H. BROWN AND MUTHUTHAMBY SRI-JAYANTHA, MEMBER, IEEE

Abstract—The design, development, and application of a research *servowriter*, which is necessary to record magnetic position encoding schemes, are presented. The servowriter is designed to evaluate emerging disk drive technologies. Submicron positioning accuracy of the disk actuator is achieved by integrating the state-of-the-art electronic, optic, electromechanical, and digital signal processing hardware. The servowriter also provides flexible and sophisticated signal encoding schemes through a programmable "pattern generator" and has several modules of customized electronic hardware, each controlled by a supervisory computer. The position of the R/W (read/write) head and actuator assembly is measured by a laser interferometric system. The measured position is used to estimate the velocity of the R/W head, which is then used to implement a state-variable-based proportional-integral-derivative controller on the Intel (8086/8087) microprocessor chip set. Both systematic and random error sources associated with phase and amplitude encoding schemes are described. Environmental factors, such as seismic vibration and temperature change, which indirectly contribute to servowriting errors, are identified and steps to contain these error sources are described.

I. Introduction

THE HIGH-performance disk drives of today are precision rotating machines, with head positioning mechanisms capable of achieving submicron track following accuracy. As the demand for track density increases, the ability to provide a higher resolution position signal will become mandatory. In order to maintain the magnetic R/W (read/write) head position along the center line of a desired track, a magnetic pattern that indicates the position of the R/W head is prerecorded on the disk surfaces during the manufacture of the disk drive. The device used to record the magnetic pattern is called a servowriter [1, p. 719]. Since the magnetic pattern helps the servo control algorithms perform the track-following or track-accessing task, it is also referred to as a servo pattern.

Of the several major steps involved in the manufacture of a disk file, the servowriting operation takes place just prior to sealing the head/disk assembly in a clean room environment. A servowriter in itself is a complex device that integrates state-of-the-art electronic, optic, and electromechanical hardware with sophisticated signal encoding schemes to achieve the submicron accuracies that are demanded in the industry. There are three broad categories of position encoding techniques used by the disk drive industry:

1) nonmagnetic position encoding (optical sensors mounted on the head actuator, mechanical detents for each track, stepper motors, etc);
2) magnetic servo pattern based position encoding (amplitude encoded schemes [2] and phase encoded schemes [3]);
3) combinations of the above (optical sensors with a single servo burst per track to remove low frequency track-following errors).

The servo control of the IBM9332, for instance, is based on a phase encoded servo pattern [4], whereas the IBM33XX series is based on an amplitude encoded servo pattern. A short overview of servo patterns is given in the Appendix.

This paper addresses the design, development, and application of a research servowriter that is targeted to achieve the magnetically based position encoding technique in category (2). Following an overview of the servowriter, its major elements are described briefly. The servowriter electronics are made up of several customized electronic hardware modules, including an Intel (8086/8087) microprocessor chip set. Each module or subsystem is associated with a function that is required to support the servowriting and testing process and is controlled by a supervisory computer (IBM-PC/AT). The pattern generator is software configurable and is controlled by the IBM-PC/AT. The IBM-PC/AT is menu driven and it is through this menu that the user controls or monitors the servowriting operation. More details are presented in [5].

The position of the R/W head is measured by a laser interferometric system [6]. The laser based position is used to estimate the state variables of the R/W head positioning mechanism. These estimates are then used to implement a state-variable-based proportional-integral-derivative (PID) controller, which positions the mechanism with zero steady-state error in the presence of bias force. Estimator/controller algorithms are implemented in 8087-based floating-point arithmetic using assembly language. An example of a closed-loop transfer function of a servowriting mechanism is presented, and factors that would contribute to track-following error, which is detrimental to the servowriter performance, are discussed.

Manuscript received March 6, 1989; revised November 6, 1989.

D. H. Brown is with IBM Applications Business Systems, Department 215, Rochester, MN 55901.

M. Sri-Jayantha is with the IBM Thomas J. Watson Research Division, Yorktown Heights, NY 10598.

IEEE Log Number 8933409.

0018-9456/90/0400-0409$01.00 © 1990 IEEE

Details related to clock pulse generation that is mandatory for locating the pattern generator pulses are described. The servo pattern is generated from 1024 × 32 bit memory-based data, thus providing flexibility to study the performance of various encoding schemes. Finally, the error sources associated with encoding schemes, and environmental factors such as seismic vibration and humidity, which indirectly contribute to servowriting errors, are identified and steps to contain these error sources are described.

II. Servowriter Description

The servo patterns are written on one or more disk surfaces, depending on the design of the file being written (i.e., dedicated versus sector servo). The servo patterns can be written with heads mounted on the disk drive actuator, or a special set of heads can be mounted to the servowriter to perform this task. The servowriting process is a repetitive process of writing a track and moving the head to the next track. The process repeats itself until all tracks are written. The process of writing the servo patterns is relatively straightforward, but since it must be precisely done, the circuitry to do this can become quite complex. Fig. 1 shows the major elements of a servowriter, some of which are briefly described now.

The heads must have a sensor mounted to them to indicate their radial position on the disk. Typically a laser interferometer is used to measure the head position. This sensor system is used in a closed-loop servo system to locate each track to be servowritten. Once the head is positioned over a track, the pattern is written. However, the pattern must be synchronized to the disk rotational position so that adjacent concentric tracks line up according to a selected encoding rule. For this task, a sensor is used to supply fine resolution clock pulses that are synchronized to the angular position of the disk. This sensor is typically a stationary R/W head called a clock head. As the spindle motor speed varies due to random disturbances, the clock pulses follow the speed changes accordingly.

An encoder or pattern generator supplies the correct servo code to the heads for writing on the disk. This pattern generator follows the angular position clock as it writes each track so that the servo pattern on that track is aligned to the servo pattern that was written on the previous adjacent track. The pattern generator is programmed to change the code written on each track so that the servo signal on read back will indicate over which track the head is positioned.

Each subsystem, together with the tasks performed by it, is coordinated by a central supervisory computer. A suitable architecture is used to share the computing, control, and monitoring tasks required by a servowriter.

III. Major Elements of a Servowriter

A. Computer Architecture

Fig. 2 shows the microprocessor hardware interconnection necessary to achieve the servowriting operation. The

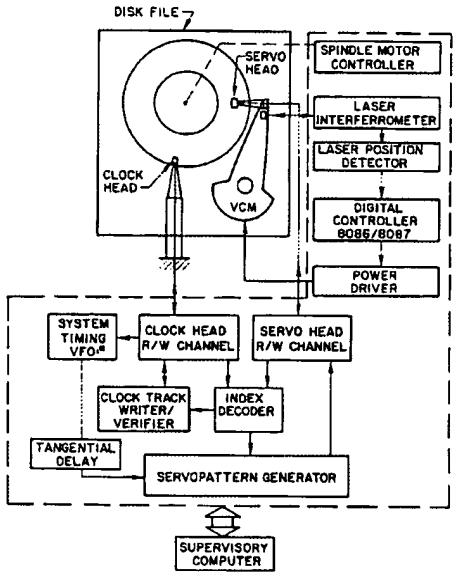

Fig. 1. Elements of a servowriter (* VFO: variable frequency oscillator).

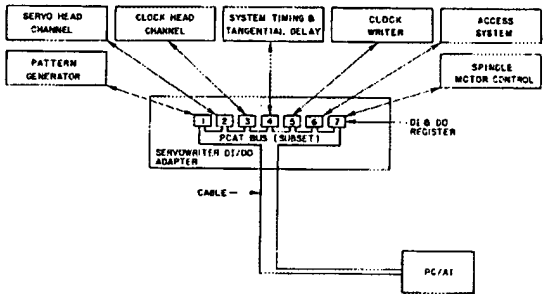

Fig. 2. Computer architecture.

servowriter is controlled by an IBM PC/AT with external data output (DO) and data input (DI) registers. The control program for this servowriter was written in IBM interpreter BASIC with some data manipulation programs (such as the pattern generator down-loader) written in 8088 Assembly language. The memory in the PC/AT is 640 kilobytes. However, the program to control the servowriter is contained in a 64 kilobyte segment. Although interpreter BASIC is slow compared to Assembly language, 2000 servo half tracks can be written on a disk in well under 1 h. This is considered adequate for a research servowriter, but is not acceptable for a production servowriter. The software would have to be optimized to reduce that time by a factor of at least 5.

B. Digital Position Control System

The head is positioned by mounting a retroreflector to the actuator and tracking it using laser interferometry. A closed-loop digital servo feedback system is employed to hold the head position to within a few microinches of the

target position. A second-order actuator model with an augmented position integral state is used for controller design. A moving coil actuator with a current-mode driver is thus modeled as follows:

$$\begin{bmatrix} x_1 \\ x_2 \\ x_3 \end{bmatrix} = \begin{bmatrix} 0 & 0 & 1 \\ 1 & 0 & 0 \\ -k_S/m & 0 & -c_S/m \end{bmatrix} \begin{bmatrix} x_1 \\ x_2 \\ x_3 \end{bmatrix} + \begin{bmatrix} 0 \\ 0 \\ k_F/m \end{bmatrix} u + \begin{bmatrix} 0 \\ -1 \\ 0 \end{bmatrix} x_{\text{Ref}} + w \quad (1)$$

$$z = [k_s \;\; 0 \;\; 0 \;\; 0]x + v \quad (2)$$

where

- c_S damping constant (N · s/m),
- k_F actuator force constant (N/A),
- k_S stiffness constant (N/m),
- k_s sensor gain constant (laser counts/m),
- m equivalent actuator mass (kgr),
- u control current commanded by servowriter processor (A),
- v laser measurement noise (equivalent laser count),
- w process noise vector (appropriate units),
- x^T [position (m), integral (m · s), velocity (m/s)],
- x_{Ref} reference position (m),
- z measured position (laser counts).

The representative model defined by (1) is used to design a PID-type controller using a pole-placement design technique. The introduction of process and measurement noise terms emphasizes that the system is not deterministic, and that the tracking performance, therefore, can never be ideal (i.e., zero error). The unmodeled disturbances act through the process noise term, w, and measurement noise appears through the noise term, v. Seismic (or ground) vibration not only affects the accuracy of the model defined by (1), but also contributes to measurement noise by causing the laser optics to move relative to the actuator. Isolation of these sources contributes significantly to the cost of a servowriter.

The continuous model is discretized for controller/estimator design. A sampling rate of 300 μs is used to discretize the model and is represented as follows (ignoring noise terms, and setting $x_{\text{Ref}} = 0$):

$$x_{k+1} = \Phi x_k + \Gamma u_k \quad (3)$$

$$z_k = h^T x_k \quad (4)$$

where

- k sample index,
- h measurement matrix as defined in (2).

Equations (3) and (4) are used to select the controller feedback gain constants. A third-order Butterworth pole pattern is used to locate the desired closed-loop poles of the position servo.

Since the measured position (i.e., laser count) is not a continuous variable, a reduced order "current" estimator is designed to obtain the velocity estimate [7, p. 149]. In the design of the estimator, measured position is assumed to be exact, and the position (error) integral state is excluded from the estimator model. Therefore, the velocity estimator is of first order, and the pole-placement design yields a single gain corresponding to a desired estimator real pole location. The integral state is derived using the trapezoidal rule for integration.

The controller/estimator gains and the system matrix elements are arranged together so that each laser position measurement is used to generate an appropriate electric current command in an explicit state variable form. The controller/estimator computations are realized in floating point arithmetic. Using a Hewlett Packard 3562A dynamic signal analyzer, a closed-loop transfer function (CLTF) of an experimental system was obtained. Fig. 3 shows the measured CLTF of an integrated disk/actuator system under servowriter control. The bandwidth of this system is limited by a 400-Hz resonance mode specific to the actuator used (in which the mounting of the retroreflector accentuated the 400-Hz mode). The servowriter controller/estimator algorithm has adequate computational speed to support a closed-loop system with much higher bandwidth if the actuator modes are not a problem from a stability standpoint. The presence of the integral state provides the required low-frequency disturbance rejection. In order to suppress high-frequency disturbance, greater bandwidth with minimum CLTF peaking is recommended.

C. System Timing and Clock Writer Design

There are different methods in practice today for writing clock signals. The simplest of all methods is to let the clock writer run freely at a designed clock frequency and to dither the disk speed (because it can never be regulated perfectly at a constant speed) until *closure* (i.e., an integral number of complete clock cycles around a track) is achieved. This task is automatically performed by the clock writer in 5 to 30 s. Hence, as defined in the next paragraph, the total number of clock cycles is first selected for a given problem, and through repeated write trials, the clock signal is recorded until satisfactory closure is met.

The total number of clock cycles per track is based on four parameters that have various system implications. They are defined as follows:

- Δ servo pattern sampling period (s),
- N_{rpm} spindle motor speed (rpm),
- f_{clock} clock track frequency (MHz),
- m_{section} integer number of sectors per revolution.

The sampling time is specified to meet the performance requirements of the disk actuator servo. (Note that the servowriter laser sampling rate is independent of the disk servo sampling rate.) The spindle speed is usually determined from magnetics considerations and is set to a spec-

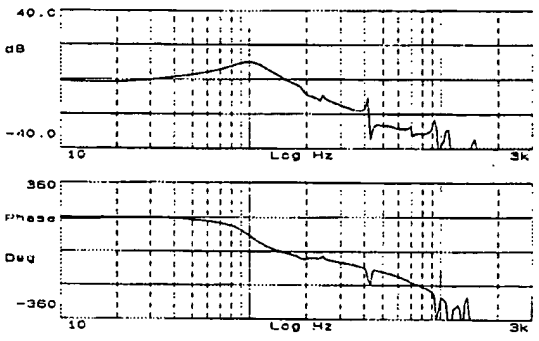

Fig. 3. Closed loop transfer function of an experimental system.

ified value. The clock frequency should meet the R/W head frequency characteristics as well as the requirements imposed by the specific servo encoding scheme. The number of sectors is, however, constrained by the relationship

$$m_{\text{sector}} = \frac{1}{\Delta} \times \frac{60}{N_{\text{rpm}}}. \tag{5}$$

The initial estimate of m_{sector} will not necessarily be an integer. Therefore, a convenient integral number of sectors, m^*_{sector}, corresponding to an exact, but slightly adjusted, sampling rate Δ^*, is selected as the first step. For instance, in order to drive the brushless dc spindle motor, an even number of sectors divisible by 12 (related to the number of motor poles) may be necessary. Based on the design requirements of the servo pattern, n_{sector} clock cycles at a frequency f_{clock} are to be generated between two consecutive sectors with a duration dictated by an adjusted sampling rate Δ^*. This requirement is met by the relationship

$$n_{\text{sector}} = \Delta^* \times f_{\text{clock}} \tag{6}$$

In the case where n_{sector} of (6) does not result in an integer, it may be rounded to the nearest integral value, n^*_{sector}. Fractional adjustment of clock frequency (in megahertz) would typically satisfy this constraint. Hence, the total number of clock cycles per revolution of the disk spindle is

$$n_{\text{total}} = n^*_{\text{sector}} \times m^*_{\text{sector}}. \tag{7}$$

This redefines the spindle speed to be

$$N^*_{\text{rpm}} = f_{\text{clock}} \times \frac{60}{n^*_{\text{sector}} \times m^*_{\text{sector}}} \tag{8}$$

which, though not exact, is near the desired spindle speed. For example, a consistent set of parameters would be $\Delta^* = 99.206\ \mu\text{s}$, $n^*_{\text{sector}} = 248\ [=99.206 \times 10^{-6} \times (2.5 \times 10^6)]$, $n_{\text{total}} = 248 \times 168 = 41\ 664$ clock cycles per revolution, and $N^*_{\text{rmp}} = 3600.23$ rpm, where the clock track writer is programmed to write n_{total} (=41 664) clock cycles at a frequency of 2.5 MHz. This is done by turning on the write current to the clock head while writing 2.5-MHz data to it. In order to have exactly 41 664 clocks written under the clock head, a counter must register how many cycles have been written during each revolution of the disk. When exactly 41 664 clocks have been written for one revolution (achieved by dithering the speed of the motor slightly around N_{rpm}), the write current is shut off.

Counting clock pulses during clock writing requires a reference mark to indicate precisely when the disk has turned through a single revolution. This is done by writing an index mark with the servo head before clock writing. The index decoder (see Fig. 1) monitors the readback signal from the servo head and outputs a pulse each time the index mark is detected. This pulse (called index) initially starts the clock writer counter during clock writing and resets it after each unsuccessful pass of clock writing. Clock track verification is done by simply reading back the written clock track and counting the number of clocks in one revolution. If disk defects damage one or more clock pulses, this will be reflected in the final count. An index mark is also encoded in the clock track to indicate the start of the clock track. Three cycles of 1.25-MHz frequency marker can be embedded in the clock track without seriously affecting the 2.5-MHz clock signal. This index is used to synchronize the pattern generators at the start of each servo track.

The clock track resolution of 400 ns is too coarse for writing servo patterns. A type 2 phase-locked loop (PLL) that multiplies the clock track frequency by 16 and holds the output phase of this 40-MHz signal constant with respect to the clock track is employed. The PLL output effectively subdivides the disk into 666 624 equally spaced time slots of 25 ns each.

D. Motor Speed Control

The speed control of the disk is critical during clock writing and clock read-back. If it varies too much during either clock writing or read-back, good closure will not be attained and the PLL that generates the system time base will go out of lock. This will make the writing of good servo patterns impossible. The speed of the disk is controlled by comparing motor Hall sensors (or, more accurately, the clock track signal) to a stable reference clock. For a research servowriter, the reference is derived from a high-precision (six to seven significant digits) frequency source. This is necessary for changing the number of clock cycles by a couple of counts per revolution. For 5.25- or 3.5-in disk drives, the motors are small enough in power consumption that single IC motor controllers are readily available, and with the proper compensation, they can control the motor speed to about 0.01 percent of reference speed.

E. Pattern Generator

The circuitry that writes the servo patterns on the tracks is called a pattern generator. It is usually programmable, but for servowriters with simple servo patterns it can be hardwired to write a limited number of servo codes. The pattern generator is a clock track counter that begins counting the 40-MHz PLL output clocks when the clock track index is received. At certain preprogrammed counts, the output of the pattern generator changes states to re-

verse the write current in the servo head. It is this sequence of transitions that makes up the servo code.

There are pattern generators of differing designs on the commercial test equipment market today. The pattern generator designed for a typical IBM servowriter is similar to some of the commercial ones except for instruction modifications to facilitate writing servo patterns. The output of the pattern generator is a shift register that clocks out the data with each 25-ns clock. The shift register can be loaded with 9–16 bits with each pattern generator instruction and then shifted out at the system PLL clock rate (40 MHz).

The pattern generator contains a block of memory, for example, 1024 × 32 bits. Each 32 bit word contains 3 bits of instruction op code, 3 bits to indicate the shift register data length, 16 bits of data, and 10 bits of op code modifier (i.e., subroutine call address, branch addresses, or loop count information). Although the instructions are simple, they allow the writing of any servo pattern used to date and, in most cases, all tracks for an entire disk can easily be contained in the 1024 locations.

F. Pattern Testing

Writing servo patterns on a disk at exactly the correct locations does not guarantee a correctly written disk. It is possible that defects on the surface of the disk were present and that the servo information was not recorded at those points. The recording head may have had a shorted turn or other defect that prevented the servo pattern from being written on the disk also.

The pattern test circuitry allows a read-back check to verify that a good servo pattern has been written. While the concepts and circuits for pattern testing are not difficult, this part of the servowriter is troublesome. Errors are neither black nor white. They fall into a broad range of values, many landing on the threshold that the pattern test uses to evaluate the correctness of the pattern. The result is that a particular disk defect or servo error may pass on some tests and fail on others, or it may pass on a particular servowriter and fail on another. The pattern testing spans several subsystems and the details are presented in [5].

IV. Error Sources

The servowriter errors can be either random or systematic and are the subject of the next section.

Error Mechanisms in the Servo Pattern

The phase encoded servo pattern looks at the average phase of many transitions with respect to a reference frequency (crystal). As a result, it is relatively immune to single transition defects and small amplitude variations. Ideally, the servo pattern phases should change continuously as the head position varies. Unfortunately the head gap geometry requires a discrete approximation. This approximation to a sloping phase angle is a $\delta/2$ ns discrete time shift for every 1/2 track width of position change. Because of this discrete implementation, there can be ripple in the position signal generated by the demodulator as the head is displaced. Selecting a finer discrete resolution does not solve the problem of ripple completely. Magnetic heads write tracks that are slightly wider than the width of the head gap. Each pass of the head while servowriting leaves a noise fringe field between tracks. This fringe field is a fixed width that is a bigger percentage of each track width as track spacing dimensions shrink. If quarter tracks are written with $\delta/4$ ns phase shifts, the linearity should get better (i.e., the ripple amplitude should decrease), but a larger percentage of the servo pattern would be made up of fringe field. Thus the improved linearity is more than negated by the noise induced.

In amplitude servo schemes, the demodulator output versus the actual head position becomes nonlinear as the head moves away from the track center line. This nonlinearity is very much dependent on the ratio of the head width to the track width. Thus the servo gain of the demodulator output (millivolts/micrometers) varies significantly with head width. Some amplitude servo patterns use only a single transition in each position sample. If such a transition is damaged, though, the position signal for that servo sample would be incorrect. Longer burst servo patterns overcome this problem to a great extent by averaging several redundant transitions (as shown in Fig. 6(b) in the Appendix). However, this redundancy cannot be carried too far because longer servo patterns begin to cause errors during high-speed seeks. They also consume the useful data space in files with sector servo architectures.

1) Tangential Delay: Due to the skew of the head on the rotary actuator as shown in Fig. 4, the tops of the transitions on track $N + 1$ do not line up with the bottoms of the transitions on track N as shown in Fig. 4(a). However, if the pattern written on track N is delayed slightly, they will line up as shown in Fig. 4(b). For such small adjustments, the 3-ns resolution is necessary. Besides head skew, nonradial motion of the actuator introduces a timing shift in the Y, or tangential, direction, as shown in Fig. 5. The tangential delay circuit can be programmed to a new correction factor for each radial servo track to remove these systematic errors. There is still a random delay due to the uncontrolled vibration of the clock head (δx_{clock}) and the servo head suspension (δy_{servo}). These two random components are time dependent, and are shown along the X and Y direction for simplicity. The effect of random vibration can be reduced by special treatment of the head suspensions or by selecting low jitter heads. Fig. 5 shows a generalized delay generating mechanism relating the track spacing (δr), radius (r), disk rotational velocity (ω), and slope of the actuator path (dy/dx). The relative time delay of a second track written next to an ideal first track (i.e., no head vibration) can be shown to be

Relative Delay

$$:= [\tau \times \delta r] + \frac{\left((\delta y_{\text{servo}} - \delta x_{\text{clock}}) + \frac{dy}{dx}\delta r\right)}{r\omega} \quad (9)$$

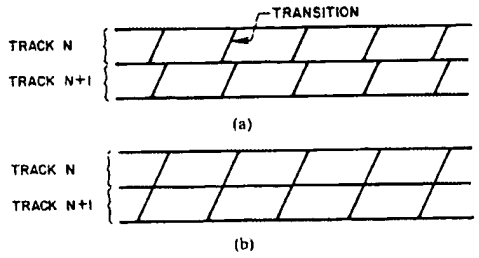

Fig. 4. Transitions with and without tangetial delay correction. (The edge of a transition can either be orthogonal or inclined (as shown) to the track centerline.) (a) Without tangetial delay correction the transitions do not line up track to track. (b) With tangential delay correction the transitions do line up with adjacent tracks.

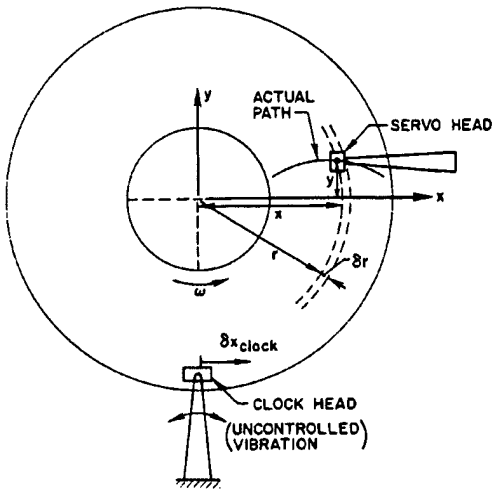

Fig. 5. Effect of nonradial head motion on tangential delay.

where τ is the ideal delay per unit distance of r. Therefore, the first group of terms in the right-hand side of (9) represents the desired ideal time delay. However, in practice the parameters defined in the second group of terms also contribute to the total delay. Observe that the delay parameters become more complicated when the actuator travels at higher velocity, as in the case of a seek.

2) Spindle and Head Suspension Jitter: As pointed out above, track to track timing alignment is essential. Mechanical movement of the spindle center line as it rotates will cause the disks to shift the track center line continually under the servowriter heads, even if the access system holds the heads perfectly stationary. Radial nonrepeatable spindle motion can cause the servo pattern being written to squeeze toward one of the adjacent tracks. Tangential nonrepeatable spindle motion can cause the data to be written out of alignment with the adjacent track, even if the timing signals were to occur at the proper times. Head suspension jitter can cause symptoms similar to spindle jitter. The head suspension jitter comes from both the clock head and the servowriting head. The jitter primarily occurs at right angles to the head suspension's main axis, as the stiffness of the suspension is weakest in that direction. In-line heads reduce tangetial jitter.

3) Vibration Isolation and Mechanical Alignment: In order to minimize file vibration during servowriting, the file is isolated from external vibrations by mounting it on a large granite base that floats on air isolation mounts. Ideally, the file should be clamped at three points, so that the base casting is not distorted while servowriting. In practice, bending modes of the casting sometimes can occur with just three clamps holding the file down and these vibrations can be written into the servo pattern in the form of track positioning errors. Thus some experimentation will usually have to be done to determine the best clamping arrangement for a particular disk drive.

The alignment of the disk and head stack for sector servowritten files is critical. During file operation, all heads on an actuator should be centered over the same track number on each surface. In addition, the servo patterns on all surfaces should pass under the heads at the same time. At the time of servowriting, this alignment is verified. However, if the file is clamped incorrectly in the servowriter or in the final product configuration, the actuator and disk spindle will tilt, resulting in radial misalignment and timing shifts from head to head. Sector servo files are designed to allow for some radial and timing misalignment, but typically these numbers are on the order of 5 μm and 500 ns, respectively.

4) Environment: The key to successful servowriting is cleanliness and the precise placement of servo information. For this reason, the environment of the servowriter is extremely important. A servowriter should be in a clean room so that exposed files will not become contaminated with dirt particles. Even in a clean room, though, dirt will accumulate on any surface (although minimal). A simple cover should be placed over each open file in the clean room while it is waiting for an assembly operation or servowriting. During the servowriting operation the cover can be removed temporarily. Besides keeping dirt off of the disks and out of the head–disk assembly (HDA) enclosure before it is sealed, magnetic particles should be purged from the clean room. Temperature is critical in precision placement of the tracks. The file dimensions will shift as the temperature changes, so it is best to keep the temperature between 68 and 72°F to minimize these mechanical changes and to facilitate operator comfort. Humidity should be between 40 and 60 percent. Above 60 percent, the humidity causes the servowriter to rust. Below 40 percent, static electricity begins to cause problems.

V. Conclusions

Servowriters may seem complex on the surface because many interleaved subsystems are involved. However, each subsystem is easy to understand. Because of the building block approach, the servowriter is very logically constructed. It is a precision machine that should be treated with care. Time and money spent on the development of a servowriter usually are recovered in a less expensive

product. However, a servowriter cannot be designed and developed independently of the file. The servowriter's mechanical clamping and access systems are directly tied to the mechanical design of the file. Likewise, a file may behave very poorly after servowriting if its design has not been thoroughly verified on the servowriter. However, no matter how much planning and testing are performed, inevitable adjustments to the file and servowriter do occur during development. They usually come in the areas of vibration isolation, file alignment, and actuator positioning. For this reason, mechanical design considerations in the file and servowriter should be given high priority. Enhancing either the software or the electronics alone will not compensate for mechanical design deficiencies. The environment causes problems that are not directly traceable. Magnetic particle contamination may appear once the product has left the servowriter. Errors in servowriting induced by temperature shifts or head crashes due to accumulation of debris never directly point to the cause, thus requiring anxious search for solutions, usually later during high-volume production. With care, it can be an extremely powerful analysis tool, and without it, a never-ending source of problems.

Appendix: Servo Patterns

The phase encoded servo pattern (or phase modulated servo) works on the principle of varying the relative phase of two bursts of squares waves (both at the same frequency) for each successive track. As a head crosses tracks, the phase shift between burst 1 and burst 2 for each track changes. This phase shift becomes an indicator of track position. In Fig. 6(a) the vertical dashed line represents the boundary between burst 1 and burst 2. When the head is positioned over track $N + 1$, there will be no phase shift between burst 1 and burst 2. When the head moves to track $N + 2$, there is a 90° phase shift between burst 1 and burst 2. The phase shift varies quite linearly with position for all head locations between tracks $N + 1$ and $N + 2$. Note that the pattern repeats every four tracks so that the same phase shift results when the head is over track N, $N + 4$, $N + 8$, $\cdots$. The benefits of a phase encoded pattern are that the servo signal frequency does not vary, the pattern is linear over four tracks, and single bit disk defects usually do not have a significant effect on the servo position signal, since multiple cycles are averaged.

The amplitude servo scheme is more commonly employed today. It has good linearity over track centers, but becomes nonlinear as the head moves off track center by more than 35 percent of the track width. This scheme is usually easier to demodulate and to servowrite. Amplitude servo relies on the principle that signal amplitude read by a head varies linearly as the head moves off track center. Referring to Fig. 6(b), the read-back signal amplitude from the head will be at its maximum during burst A when the head is positioned over track N, $N + 2$, $N + 4$, $\cdots$. As the head moves off track, the amplitude of the burst A signal decreases in proportion to the amount of off-track position, and burst B amplitude begins to increase from 0. At tracks $N + 1$, $N + 3$, $N + 5$, $\cdots$, the signal from burst B is at its maximum and burst A is zero. Like the phase encoded servo, this scheme will tolerate small disk defects since many cycles are used in the burst. However, amplitude servo is not as linear as a phase encoded servo and there are two widely separated frequency components in the pattern—dc and the burst frequency.

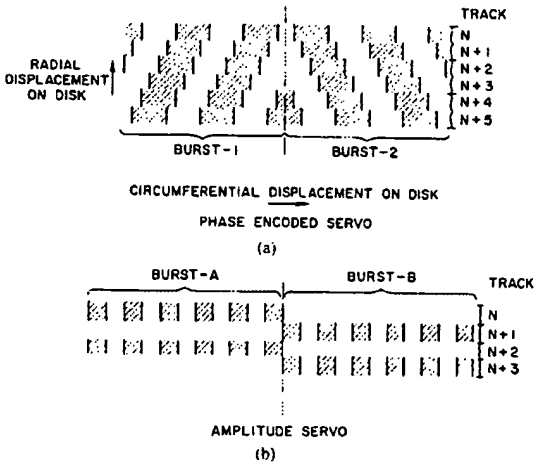

Fig. 6. (a) Phase encoded servo pattern. (b) Amplitude encoded servo pattern.

References

[1] R. B. Mulvany and L. H. Thompson, "Innovations in disk film manufacturing," *IBM J. Res. Develop.*, vol. 25, no. 5, pp. 711-723, Sept. 1981.

[2] R. K. Oswald, "Design of a disk file head-positioning servo," *IBM J. Res. Develop.*, pp. 506-512, Nov. 1974.

[3] F. E. Axmear and D. W. Collins, "Phase modulated servo systems," U.S. Patent 4 549 232, Oct. 1985.

[4] M. Stich, "Digital servo algorithm for disk actuator control," in *Proc. Conf. Appl. Motion Control (CAMC)*, June 1987, pp. 35-41.

[5] D. H. Brown and M. Sri-Jayantha, "Development of a servowriter for magnetic disk storage application," IBM Res. Report, RC 14187, Yorktown Heights, NY, Nov. 1988.

[6] *HP Laser Transducer System: System Operating and Service Manual*, Hewlett Packard Company, CA, Nov. 1974.

[7] G. Franklin and J. D. Powel, *Digital Control of Dynamic Systems*, Reading, MA: Addison-Wesley, 1981.

H_∞ speed control of an induction motor with the two-mass resonant system by LMI

Jin-Soo Kim Young-Seok Kim Jae-Hwa Shin Hyun-Jung Kim
Dept. of Electr. Eng., Inha Univ., Inchon, South Korea;

This paper appears in: **Industrial Electronics Society, 1998. IECON '98. Proceedings of the 24th Annual Conference of the IEEE**

Meeting Date: 08/31/1998 - 09/04/1998
Publication Date: 31 Aug.-4 Sept. 1998
Location: Aachen Germany
On page(s): 1439 - 1444 vol.3
Volume: 3
Reference Cited: 10
Number of Pages: 4 vol. xxix+2635
Inspec Accession Number: 6142330

Abstract:
In industrial motor drive systems, a shaft torsional **vibration** is often generated when a motor and a load are connected with a flexible shaft. This paper treats the **vibration** suppression control of such a system. In this paper, a control system design method using linear matrix inequality (LMI), which is a tool for control design that replaces or complements Lyapunov-**Riccati** equations, is provided and the H_∞ speed controller for an induction motor by LMI is proposed. In the H_∞ speed controller, weights are used to satisfy tracking and disturbance rejection. Experimental results show the validity of the proposed H_∞ speed controller by LMI, and this controller is compared with the state feedback controller

Index Terms:
H&infin control control system synthesis induction motor drives machine control machine testing machine theory variable speed drives velocity control **vibration** control H_{∞} speed control Lyapunov-**Riccati** equations control design control performance disturbance rejection induction motor industrial motor drive system linear matrix inequality shaft torsional **vibration** state feedback controller tracking two-mass resonant system **vibration** suppression control

Documents that cite this document

There are no citing documents available in IEEE Xplore at this time.

Search Results [PDF FULL-TEXT 340 KB] PREV NEXT DOWNLOAD CITATION

Home | Log-out | Journals | Conference Proceedings | Standards | Search by Author | Basic Search | Advanced Search | Join IEEE | Web Account | New this week | OPAC Linking Information | Your Feedback | Technical Support | Email Alerting | No Robots Please | Release Notes | IEEE Online Publications | Help | FAQ| Terms | Back to Top

H_∞ Speed Control of an Induction Motor with the Two-Mass Resonant System by LMI

Jin-Soo Kim
Dept. of E. E.
Inha University
253 Yonghyun-dong
Nam-ku, Inchon
402-751, Korea
g9541959@inhavision.inha.ac.kr

Young-Seok Kim
Dept. of E. E.
Inha University
253 Yonghyun-dong
Nam-ku, Inchon
402-751, Korea
youngsk@dragon.inha.ac.kr

Jae-Hwa Shin
Dept. of Electric
Junior College of Inchon
235 Tohwa-dong
Nam-ku, Inchon
402-750, Korea
shinjh@falcon.icc.ac.kr

Hyun-Jung Kim
Dept. of Control & Instrumentation
Yuhan Junior College
185-34, Koean-dong
Puchon, Kyongki-Do
422-749, Korea
kimhj@green.yuhan.ac.kr

Abstract - **In the industrial motor drive system, a shaft torsional vibration is often generated when a motor and a load are connected with a flexible shaft. This paper treats the vibration suppression control of such a system. In this paper, a control system design method using Linear Matrix Inequality (LMI), which is a tool for control design that replaces or complements Lyapunov-Riccati equations, is provided and the H_∞ speed controller for an induction motor by LMI is proposed. In the H_∞ speed controller, weights are used to satisfy tracking and disturbance rejection. Experimental results show the validity of the proposed H_∞ speed controller by LMI, and this controller is compared with the state feedback controller.**

1. Introduction

In the industrial motor drive systems such as industrial robots, rolling mills, elevators and so on, the shaft torsional vibration is often generated when a motor and a load are connected with a flexible shaft. Such a system is called as the two-mass resonant system and this paper treats the vibration suppression control of this system.

To suppress the shaft torsional vibration, the resonant ratio control, the state feedback control, the LQG control and the H_∞ control are studied.[1~6] It is often impossible to detect the load speed, the shaft torsional torque and the load disturbance torque in the real systems. Recently, it is studied the new method which estimates unknown state variables by using the reduced order observer and feed back these state variables by using the pole placement design method.[7] But this design method doesn't satisfy the fast speed response property and the attenuation property of load disturbance at the same time.

In recent studies, there is the H_∞ control which satisfies the fast speed response property and the attenuation property of load disturbance at the same time by using the weights. The H_∞ control is often applied in the industrial systems.

In recent, because it is possible to represent the control specifications and the robust stable conditons by Linear Matrix Inequality (LMI), the control problem can be transformed into the convex problem.[8,9] LMIs have gained much attention as a tool for control design that replaces or complements Lyapunov-Riccati equations.

In this paper, the controller design method by LMI is provided and the H_∞ speed controller of an induction motor by LMI is proposed. The validity of the proposed controller is comfirmed by experimental results and this controller is compared with the conventional state feedback controller using the pole placement method.[7]

2. The two-mass resonant system

The two-mass resonant system which has a motor and a load connected with a flexible shaft is shown in fig. 1. The state equation of the two-mass resonant system is as follows

$$\begin{bmatrix} \dot{\omega}_M \\ \dot{\omega}_L \\ \dot{T}_{SH} \end{bmatrix} = \begin{bmatrix} -\frac{B_M}{J_M} & 0 & -\frac{1}{J_M} \\ 0 & -\frac{B_L}{J_L} & \frac{1}{J_L} \\ K_{SH} & -K_{SH} & 0 \end{bmatrix} \begin{bmatrix} \omega_M \\ \omega_L \\ T_{SH} \end{bmatrix}$$

0-7803-4503-7/98/$10.00 1998 IEEE

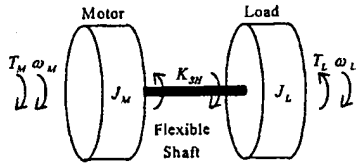

Fig.1 The plant model of the two-mass resonant system

$$+\begin{bmatrix} \frac{1}{J_M} & 0 \\ 0 & -\frac{1}{J_L} \\ 0 & 0 \end{bmatrix}\begin{bmatrix} T_M \\ T_L \end{bmatrix} \quad (1)$$

where,

J_M, J_L : the motor inertia, the load inertia

B_M, B_L : the motor viscous damping coefficient, the load viscous damping coefficient

K_{SH} : the shaft stiffness

ω_M, ω_L : the motor speed, the load speed

T_M, T_{SH}, T_L : the motor torque, the shaft torsional torque, the load disturbance torque

The goals for the control of the two-mass resonant system are stated in the following forms.

(1) Suppress the shaft torsional vibration.

(2) Reject the effect of the load disturbance torque.

(3) For the change of the speed reference, the load speed follows it quickly without overshoot.

3. The H∞ generalized plant

Fig. 2 is the H∞ generalized plant to apply the H ∞ control theory to the two-mass system. In fig. 2, w_1, w_2 are inputs for disturbance and command, respectively. and z_1, z_u are outputs. z_1 is as follows.

$$z_1 = C_z x = \begin{bmatrix} \omega_M \\ \omega_M - \omega_L \\ \omega_L \end{bmatrix}, C_z = \begin{bmatrix} 1 & 0 & 0 \\ 1 & 0 & -1 \\ 0 & 0 & 1 \end{bmatrix} \quad (2)$$

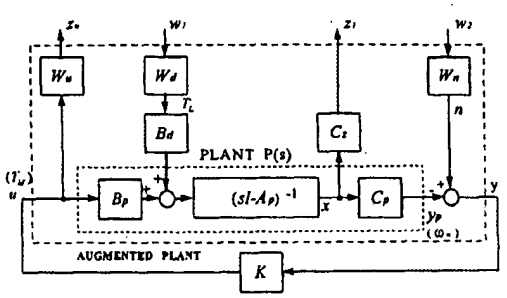

Fig. 2 The generalized plant of the H∞ control

T_L is the disturbance torque and n is the speed command. W_d is weight for T_L and W_n is weight for n. If weights are defined as follows,

$$W_d = \begin{bmatrix} A_{Wd} & B_{Wd} \\ C_{Wd} & D_{Wd} \end{bmatrix},$$

$$W_n = \begin{bmatrix} A_{Wn} & B_{Wn} \\ C_{Wn} & D_{Wn} \end{bmatrix}, W_u = D_{Wu} \quad (3)$$

then the state space equation for the generalized plant and the ratio of output to input, G, are as follows.

$$\begin{bmatrix} \dot{x} \\ z \\ y \end{bmatrix} = \begin{bmatrix} A & B_1 & B_2 \\ C_1 & 0 & D_{12} \\ C_2 & D_{21} & 0 \end{bmatrix}\begin{bmatrix} x \\ w \\ u \end{bmatrix} \quad (4)$$

$$G := \begin{bmatrix} A & B_1 & B_2 \\ C_1 & 0 & D_{12} \\ C_2 & D_{21} & 0 \end{bmatrix} = \begin{bmatrix} A_p & 0 & B_d C_{Wd} & 0 & B_d D_{Wd} & B_p \\ 0 & A_{Wn} & 0 & B_{Wn} & 0 & 0 \\ 0 & 0 & A_{Wd} & 0 & B_{Wd} & 0 \\ C_z & 0 & 0 & 0 & 0 & 0 \\ 0 & 0 & 0 & 0 & 0 & D_{Wu} \\ -C_p & C_{Wn} & 0 & D_{Wn} & 0 & 0 \end{bmatrix} \quad (5)$$

Above G is obtained by choice of W_d, W_n, W_u and the H∞ controller K is solved by Matlab.

4. The control system design by LMI

In this chapter, we represent G of the generalized plant by LMI. Convexity of LMI and LMI representation of Riccati inequality for the control design are given and convex problems involving LMI are treated.

Riccati inequality applying to control system design is as follows.

$$A^TS + SA + SBR^{-1}B^TS + Q < 0 \ , \ R > 0 \qquad (6)$$

In Eq. (6), A and B are

$$A = \begin{bmatrix} A_p & 0 & B_dC_{Wd} \\ 0 & A_{Wn} & 0 \\ 0 & 0 & A_{Wd} \end{bmatrix},$$

$$B = [\, B_1 \ B_2 \,] = \begin{bmatrix} 0 & B_dD_{Wd} & B_p \\ B_{Wn} & 0 & 0 \\ 0 & B_{Wd} & 0 \end{bmatrix} \qquad (7)$$

in real two-mass system and Q, R, S can be sellected by free choice. Eq. (6) can be transformed into

$$\begin{bmatrix} -A^TS - SA - Q & SB \\ B^TS & R \end{bmatrix} = F(e) > 0 \qquad (8)$$

by using Schur complement.[10] And Eq. (8) can be converted to following general form of LMI.

$$F(e) = F_0 + \sum_{i=1}^{m} e_iF_i \qquad (9)$$

where

$$F_0 = \begin{bmatrix} -Q & 0 \\ 0 & R \end{bmatrix}, \quad F_i = \begin{bmatrix} -A^TS_i - S_iA & S_iB \\ B^TS_i & 0 \end{bmatrix},$$

e_i : vector

Convex problems for solving $F(e) > 0$ are remarkably two problems as follows.

1) Convex Feasibility Problem (CFP)
find $e \in \mathcal{R}^m$ such that $F(e) > 0$
2) Convex Minimization Problem (CMP)
minimize c^Te subject to $F(e) > 0$, $e \in \mathcal{R}^m$
where $c \in \mathcal{R}^m$ is given.

And because of scaled matrix norm condition, $\| WFW^{-1} \| < \gamma$, can be transformed into eq. (10),

$$\| WFW^{-1} \| < \gamma \Leftrightarrow W^{-T}F^TW^TWFW^{-1} < \gamma^2 I$$
$$\Leftrightarrow F^TW^TWF < \gamma^2 W^TW$$
$$\Leftrightarrow \gamma^2 V - F^TVF > 0; \ V := W^TW > 0 \qquad (10)$$
where W : scaling matrix, γ : level

following problems can be obtained.

1) CFP : when matrix F and level $\gamma > 0$ are given, problem solving scaling matrix W(or V);
$\exists\, V := W^TW > 0$ such that $\gamma^2 V - F^TVF > 0$
2) CMP : when matrix F and scaling matrix W are given, problem minimizing level γ;
minimize $\gamma > 0$ such that $\gamma^2 V - F^TVF > 0$

We can get W(or V) in case of minimum γ by iteration.

5. H_∞ speed control of the two-mass system by LMI

We design the H_∞ controller of the two-mass system by LMI. In fig. 3, the weighting function W_u is selected as $W_u = 10^{-6}$ which does not influence the design of controller. The choice of weighting functions is very critical because the control performances are determined by weighting functions. The weighting function W_d is for the closed-loop transfer function from the disturbance torque T_L to z_1. In order to achieve the design specifications such as vibration suppession and disturbance rejection, $|W_d|^{-1}$ is chosen as closed-loop gain plot of the one-mass system. The weighting function W_n is for the closed-loop transfer function from the disturbance torque n to z_1, where n corresponds to the speed command or noise. The closed-loop transfer function from n to ω_M is a complementary sensitivity function, so W_n is chosen as a high pass filter considering the robust stability. Then W_d and W_n are chosen as follows.

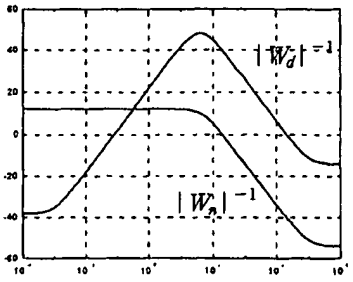

Fig. 3 Bode diagram of weights
(ver : [dB], hor : [ω])

$$W_d = \gamma_d \frac{(s+\omega_d)}{(s+10^{-3})(s+10^5)},$$

$$W_n = \gamma_n \frac{(s+50)}{(s+10^5)} \tag{11}$$

The H_∞ controller $K(s)$ can be obtained by using Matlab after adjusting the parameters in weighting functions as $\gamma_d = 5$, $w_d = 40$, $\gamma_n = 500$. Weighting functions are shown in fig. 3. The H_∞ controller $K(s)$ is given by

$$K(s) = 4.921\times10^4 \times \frac{(s+1\times10^5)(s+0.6\pm j80)(s+5.41)}{(s+5.6\times10^5)(s+3.59\times10^4)(s+9\pm j33.52)(s+0.0011)} \tag{12}$$

6. Experimental system

The configuration of the experimental system for the two-mass resonant system is shown in fig. 4. There is a flexible shaft (l : 800 [mm], ϕ : 13 [mm]) between a motor and a load generator. This system is used variable inertia to change the inertia of a motor or a load generator. For this paper, it is only used variable inertia for a load generator. The mechanical constants of the two-mass resonant system are listed on Table 1.

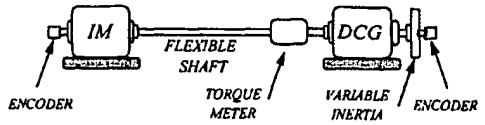

Fig. 4 The experimental system for the two-mass resonant system

Table 1 The mechanical constants of the two-mass resonant system

J_M	J_L	K_{SH}
0.008 [kgm^2]	0.08 [kgm^2]	50.527 [Nm/rad]

7. Experimental results

Experimental results show the validity of the proposed controller and this controller is compared with the state feedback controller. The inertia ratio is 0.008 : 0.08 (J_M : J_L) in this paper. Experiments are composed of speed response experiment and load disturbance response experiment.

7.1. Speed response experiment

The reference speed of the load is 200[rpm] as a step input at 0 [sec]. Fig. 5, 6 are experimental results of step response under the state feedback control. Fig. 5 shows load speed and motor speed and fig. 6 shows shaft torsional torque. The speed transient time from 0 to 200 [rpm] is about 0.7 [sec]. If the transient time becomes shorter, overshoot of the load speed is larger. In the transient time, maximum torque is 6 [Nm].

Fig. 7, 8 are experimental results for control by LMI. Because the speed transient time from 0 to 200 [rpm] is about 0.5 [sec], the transient time of proposed LMI controller has much less than that of state feedback controller. This is because of adjusting the weighting function for speed response. In the transient time, maximum torque is 9 [Nm]. But this maximum torque does not influence the two-mass system.

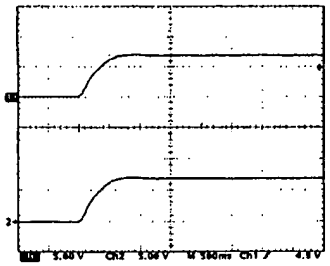

Fig. 5 State feedback controller
150 [rpm]/div, 0.5 sec/div
(upper) Real motor speed, (down) Real load speed

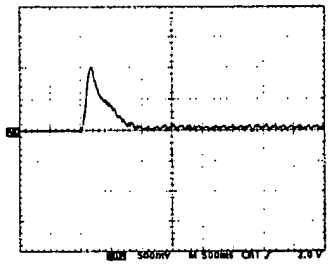

Fig. 6 State feedback controller
3 [Nm]/div, 0.5 sec/div
Real shaft torsional torque

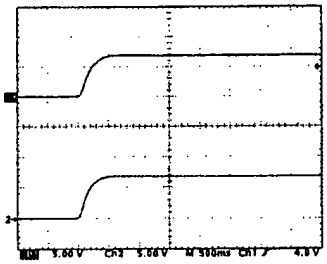

Fig. 7 LMI controller
150 [rpm]/div, 0.5 sec/div
(upper) Real motor speed, (down) Real load speed

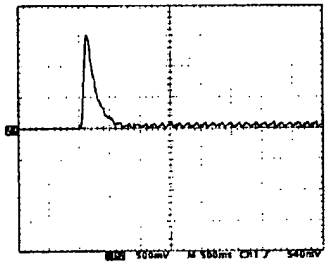

Fig. 8 LMI controller
3 [Nm]/div, 0.5 sec/div
Real shaft torsional torque

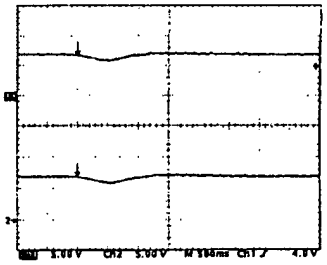

Fig. 9 State feedback controller
150 [rpm]/div, 0.5 sec/div
(upper) Real motor speed, (down) Real load speed

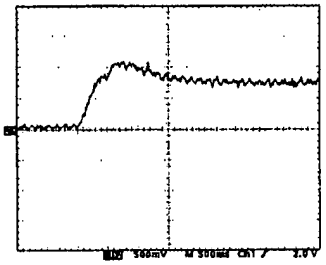

Fig. 10 State feedback controller
3 [Nm]/div, 0.5 sec/div
Real shaft torsional torque

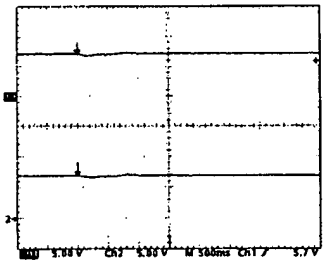

Fig. 11 LMI controller
150 [rpm]/div, 0.5 sec/div
(upper) Real motor speed, (down) Real load speed

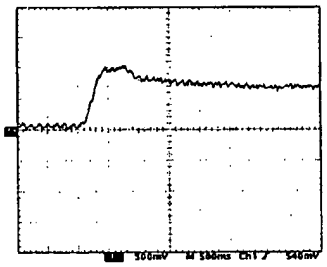

Fig. 12 LMI controller
3 [Nm]/div, 0.5 sec/div
Real shaft torsional torque

7.2. Load disturbance response experiment

A resistor load which can be connected with DC generator is used as a load. By using a resistor load, the load disturbancs torque is increased from 0 to 4.5 [Nm] at 200 [rpm]. 4.5 [Nm] is 37% of rated torque. Fig. 9, 10 are experimental results for the state feedback control. Load speed dropped 17% of 200 [rpm] and recovered after 1.2 [sec]. This is because the inertia ratio is big. If the inertia ratio increases, the recovery time is much longer.

Fig. 11, 12 are experimental results for control by LMI. The load speed dropped 5% of 200 [rpm] and recovered after 0.6 [sec]. Then, the speed drop of the proposed LMI controller has much less than that of state feedback controller. The recovery time of the proposed LMI controller has much less than that of the state feedback controller.

8. Conclusion

This paper treated the speed control of the induction motor system which has a motor and a load connected with a flexible shaft. The H_∞ speed control of an induction motor with two-mass resonant system by LMI is proposed. In the proposed control, the H_∞ control, which satisfies the fast speed response property and the attenuation property of load disturbance at the same time by using the weights, is used and is repesented by LMI which is a tool for control design that replaces or complements Lyapunov-Riccati equations.

The experiments show the excellent performance of the proposed H_∞ speed control by LMI compared with the state feedback control.

This research was supported by the Korea Organization of Science and Engineering Foundation.(No. 951-0912-098-2)

References

[1] Yuki, Murakami, Ohnishi, "Vibration Control of a 2 Mass Resonant System by the Resonant Ratio Control", T.IEE Japan, Vol.113-D , No. 13, 1993, pp. 1162~1169

[2] Kameyama, Ohashi, Morimoto, Takeda, "Torsional Vibration Suppression by Resonance Ratio Control and Design of Controller Gains", JIASC, 1994, pp. 1150~1155

[3] Sugimoto, Morimoto, Takeda, Hirasa, "Vibration Suppression of Two-Mass System by the State Feedback Control and Control Characteristic Considering Parameter Variations", JIASC, 1993, pp. 843~848

[4] Jun-Keun Ji et. al., "LQG Based Speed Controller for Torsional Vibration Suppression in 2-Mass Motor Drive System", IEEE IECON, Vol. 2, pp. 1157~1162

[5] Morimoto, Takeda, Hirasa, "Speed Control of Two-Mass Mechanical System Based on H_∞ Control Theory", JIASC, 1993, pp. 849~854

[6] Akihiko Tanisaka et al, "Application of H_∞ Control to Motor Speed Control System", IEEE IECON, 1991, pp. 839~842

[7] Iwasaki, Hiroe, Matsui, "State Feedback Control of 2-Mass Resonant System and Parameter Measurement", JIASC, 1994, pp. 1180~1185

[8] T. Iwasaki, "Control System Design via LMIs", J.SICE, Vol. 34, No. 3, Mar. 1995

[9] S. Boyd et al., "Linear Matrix Inequalities in System and Control", SIAM, 1994, pp. 1~35

[10] Zhou, Doyle, Glover, "Robust and Optimal Control", Prentice-Hall, Inc., 1996, pp. 17~44